NASA TECHNICAL NOTE

NASA TN D-5932

NASA TN D-5932

FULL-SCALE WIND-TUNNEL INVESTIGATION OF THE AERODYNAMIC CHARACTERISTICS OF THE X-24A LIFTING BODY AIRCRAFT

by
Kenneth W. Mort
Ames Research Center

and
Michael D. Falarski
U.S. Army Aeronautical Research Laboratory

NATIONAL AERONAUTICS AND SPACE ADMINISTRATION • WASHINGTON, D. C. • AUGUST 1970

1. Report No. NASA TN D-5932	2. Government Accession No.	3. Recipient's Catalog No.
4. Title and Subtitle FULL-SCALE WIND-TUNNEL INVESTIGATION OF THE AERODYNAMIC CHARACTERISTICS OF THE X-24A LIFTING BODY AIRCRAFT		5. Report Date August 1970 6. Performing Organization Code
7. Author(s) Kenneth W. Mort and Michael D. Falarski		8. Performing Organization Report No. A-2823 10. Work Unit No. 124-07-02-34-00-21
9. Performing Organization Name and Address NASA Ames Research Center and U.S. Army Aeronautical Research Laboratory Moffett Field, California 94035		11. Contract or Grant No.
12. Sponsoring Agency Name and Address National Aeronautics and Space Administration Washington, D.C. 20546		13. Type of Report and Period Covered Technical Note 14. Sponsoring Agency Code
15. Supplementary Notes		

16. Abstract

The aerodynamic characteristics of the X-24A aircraft were investigated in the Ames 40- by 80-Foot Wind Tunnel. The aircraft was tested over an angle-of-attack range of -4° to +32°, an angle-of-sideslip range of -6° to +6°, for several longitudinal, lateral, and directional control settings, and for Reynolds numbers ranging from 20.7×10^6 to 41.6×10^6. (Most of the data were obtained at a Reynolds number of 32.4×10^6.) Results were obtained with the landing gear both up and down. With the landing gear up the maximum lift-to-drag ratio achieved was 5.2 untrimmed and 4.4 trimmed. With the landing gear down the maximum trimmed L/D was lower by an amount which varied from 0.8 to 1.8, depending on the upper flap deflection. In flight, lowering the landing gear would require a longitudinal control change of 7° to 10°, depending on the angle of attack, to maintain a constant lift coefficient or forward velocity. A limited comparison with 1/5 scale-model longitudinal results showed very good agreement.

17. Key Words (Suggested by Author(s))	18. Distribution Statement
Lifting body Subsonic aerodynamics, aircraft Subsonic aerodynamics, missiles and space vehicles	Unclassified - Unlimited

19. Security Classif. (of this report)	20. Security Classif. (of this page)	21. No. of Pages	22. Price *
UNCLASSIFIED	UNCLASSIFIED	58	$3.00

*For sale by the Clearinghouse for Federal Scientific and Technical Information
Springfield, Virginia 22151

NOTATION

b	reference span, 10 ft
C_D	drag coefficient, $\frac{D}{qS}$
C_l	rolling-moment coefficient, $\frac{\text{rolling moment}}{qSb}$
C_L	lift coefficient, $\frac{L}{qS}$
C_m	pitching-moment coefficient, $\frac{\text{pitching moment}}{qSl}$
C_n	yawing-moment coefficient, $\frac{\text{yawing moment}}{qSb}$
C_y	side-force coefficient, $\frac{\text{side force}}{qS}$
D	drag force, lb
l	reference length, 23 ft
L	lift force, lb
q	free-stream dynamic pressure, psf
R	Reynolds number, $\frac{Vl}{\text{kinematic viscosity}}$
S	reference area, 162 ft^2
V	free-stream velocity, fps
α	angle of attack, referenced to lower surface (see fig. 2(a)), deg
β	angle of sideslip (see fig. 2(a)), deg
δ_a	differential flap deflection, (left side) - (right side), deg
δ_u	average deflection of upper flaps, deg
δ_l	average deflection of lower flaps, deg
δ_r	average rudder deflection, deg
δ_{rf}	average flare of all four rudder sections, deg

All control deflections were measured in a plane perpendicular to the control hinge line. See figure 3 for the sign conventions and figure 2(c) for the reference position for all controls except the rudders, which are referenced to the flared position.

The data presented are referred to the wind axes for all force coefficients and to the body axes for all moment coefficients.

FULL-SCALE WIND-TUNNEL INVESTIGATION OF THE AERODYNAMIC CHARACTERISTICS OF THE X-24A LIFTING BODY AIRCRAFT*

Kenneth W. Mort
Ames Research Center

and

Michael D. Falarski
U.S. Army Aeronautical Laboratory

SUMMARY

The aerodynamic characteristics of the X-24A aircraft were investigated in the Ames 40- by 80-Foot Wind Tunnel. The aircraft was tested over an angle-of-attack range of -4° to +32°, an angle-of-sideslip range of -6° to +6°, for several longitudinal, lateral, and directional control settings, and for Reynolds numbers ranging from 20.7×10^6 to 41.6×10^6. (Most of the data were obtained at a Reynolds number of 32.4×10^6.) Results were obtained with the landing gear both up and down. With the landing gear up the maximum lift-to-drag ratio achieved was 5.2 untrimmed and 4.4 trimmed. With the landing gear down the maximum trimmed L/D was lower by an amount which varied from 0.8 to 1.8, depending on the upper flap deflection. In flight, lowering the landing gear would require a longitudinal control change of 7° to 10°, depending on the angle of attack, to maintain a constant lift coefficient or forward velocity. A limited comparison with 1/5 scale-model longitudinal results showed very good agreement.

INTRODUCTION

Many studies have been conducted in developing lifting reentry vehicles (lifting bodies) capable of gliding to a specified recovery site, and of making a horizontal landing. Flight vehicles using three different configurations have been built to investigate atmospheric flight characteristics prior to and during the landing maneuver. Two of these configurations were designated M2-F2 and HL-10. (See ref. 1 for results of flight testing the M2-F2 and refs. 2 and 3 for results of wind-tunnel testing the M2-F2 and HL-10.) The third configuration is the X-24A lifting body. Wind-tunnel tests were performed on a 1/5 scale model of the X-24A configuration and the results were reported in reference 4. To determine if scale and viscous effects at full-scale Reynolds numbers introduced unacceptable aerodynamic characteristics, the X-24A aircraft was tested in the Ames 40- by 80-Foot Wind Tunnel. Results of this investigation are presented herein.

VEHICLE DESCRIPTION

The X-24A aircraft is shown in figure 1 installed in the test section of the Ames 40- by 80-Foot Wind Tunnel. Dimensions and geometry are given in figure 2. The aircraft had upper flaps that could be moved together for longitudinal control and differentially for lateral control and lower flaps that could also be moved together for longitudinal control and differentially for lateral control. The sign convention used for the control surface deflections is illustrated in figure 3. As shown in figure 2(c) the vehicle also had two sets of rudders, an upper set and a lower set. The control system of the aircraft was designed to use the lower flaps for longitudinal and lateral control and the upper rudders for directional control. However, the effects of all the control surfaces were included in the investigation.

TEST PROCEDURE

The aerodynamic characteristics were obtained by setting dynamic pressure and sideslip angle and varying either angle of attack or control position. The effects of Reynolds numbers from 20.7×10^6 to 41.6×10^6 were determined at one longitudinal control setting and zero sideslip. The effects of Reynolds number at this condition were found to be small and were assumed to be small at other test conditions. Therefore, the remainder of the investigation was performed at a Reynolds number of 32.4×10^6 (dynamic pressure of about 59 psf). Testing was performed with the landing gear both up and down. The mounting arrangement with the gear up is shown in figures 1(a) and 1(b) and with the gear down in figures 1(c) and 1(d).

REDUCTION OF DATA

Corrections

No tunnel-wall corrections were applied to the data presented since the estimated magnitude of these corrections indicated they were insignificant.

The data were corrected for tares due to the unshielded portion of the struts (see fig. 1(a)). These tares were obtained in the following manner. The lower sections of the forward unshielded struts were tested while mounted on the tunnel support struts without the aircraft or upper sections of the struts. (The entire unshielded section of the rear strut was tested in this manner.) The upper sections of the forward unshielded struts were tested while suspended from the aircraft with the aircraft mounted as shown in figure 1(e). (The upper section of the strut is not shown in this figure.) Therefore the tares include the interaction between the struts and aircraft and the interaction between the fairings and struts. (The effects of the free ends during the tare testing were not accounted for; however, estimates indicate that they were small.) With the landing gear up the

tare values used were: $\Delta C_L = -0.054 \sin \alpha$, $\Delta C_D = 0.045 - 0.048 \sin \alpha$, and $\Delta C_m = -0.006$; with the landing gear down the values were: $\Delta C_D = 0.012$ and $\Delta C_m = -0.0036$. (All of these coefficients are referred to the wind axes.)

Accuracy of Measurement

The various quantities measured were accurate within the following limits which include error limits involved in calibrating, reading, and reducing the data.

Angle of attack	±0.2°
Angle of sideslip	±0.5°
Free-stream dynamic pressure	±1/2 percent
Control surface settings	±0.5°

	Force or moment	Coefficients at $R = 32.4 \times 10^6$ (q = 59 psf)
Lift	±5 lb	±0.00052
Drag	±3 lb	±0.00031
Side force	±3 lb	±0.00031
Pitching moment	±200 ft-lb	±0.00091
Yawing moment	±100 ft-lb	±0.00105
Rolling moment	±300 ft-lb	±0.00314

RESULTS

Table 1 is a complete index of plotted test results. The data presented in figures 4 through 9 show the effects on the basic longitudinal aerodynamic characteristics of the following parameters: Reynolds number (fig. 4); upper and lower flap setting for three rudder flare settings with the landing gear up (figs. 5, 6, and 7); upper and lower flap setting with the landing gear down (fig. 8); and angle of sideslip (fig. 9). Also shown is a comparison with the 1/5 scale model results of reference 4 (fig. 10). Longitudinally trimmed characteristics determined from figures 5 through 8 are shown in figure 11. Figure 11(a) shows the effect of upper flap deflection, figure 11(b) the effect of rudder flare, and figure 11(c) the effect of the landing gear.

The lateral-directional aerodynamic characteristics are presented in figures 12 through 16. These figures show the effects of varying sideslip angle and angle of attack (fig. 12); upper rudder deflection (fig. 13); lower rudder deflection (fig. 14); differential upper flap deflection (fig. 15); and differential lower flap deflection (fig. 16). These results were investigated for upper flap settings

from -15° to -30°, lower flap settings from 10° to 30°, and rudder flare angles of -9°, 0°, and 9° for all controls except the lower rudders. The aerodynamic characteristics of the lower rudders were only examined with the landing gear down, upper flaps at -20° and -30°, lower flaps at 20°, and rudder flare of 0°. The results are presented for these ranges only if there were significant effects of these variables.

DISCUSSION

Longitudinal Aerodynamic Characteristics

The effect of Reynolds number was examined for an upper flap setting of -20°, a lower flap setting of +10°, and a rudder flare setting of -9° with the landing gear up. From the results shown in figure 4, it is evident that for the range investigated the effect of Reynolds number was small. In view of this it was assumed that the effects of Reynolds number would be small at other test conditions and hence the remaining results were obtained at one Reynolds number, 32.4×10^6 (dynamic pressure of 59 psf).

Comparison with 1/5 scale model of reference 4— The longitudinal aerodynamic characteristics of the aircraft (extrapolated to -10° δ_{rf} using data from figs. 5(a) and 6(a)) and a 1/5 scale model (ref. 4) are compared in figure 10 for an upper flap setting of -5°, a lower flap setting of 0°, and a rudder flare setting of -10°. Agreement is good; the only significant differences, which are small, are a shift in the angle of attack required for the same lift coefficient, which is about 1°, and a shift in pitching-moment coefficient at the same lift coefficient, which is equivalent to less than 5° of lower flap setting.

Trimmed aerodynamic characteristics for the X-24A aircraft— The maximum trimmed lift-to-drag ratio (L/D) was 4.4 (fig. 11(a)), but the corresponding longitudinal control settings would not provide for an adequate longitudinal control margin for maneuvering. A usable L/D would probably range from about 3-1/2 to 4. As a point of reference, this glide performance may be compared with that achieved by the M2-F2 aircraft (ref. 2) and the HL-10 aircraft (ref. 3) which were designed for the same mission. The maximum L/D from wind-tunnel test results of these aircraft with the controls in the flight test configuration was slightly greater than 3 for the M2-F2 and about 3-1/4 for the HL-10.

Rudder flare had a large effect on the lower flap setting required for trim (fig. 11(b)). Each degree increase in rudder flare requires approximately a 1° decrease in lower flap deflection to maintain the same trimmed lift coefficient. Because of this relationship and because of the lower flap travel limitations, large reductions in the maximum-trimmed lift coefficient occurred with increasing rudder flare. The more negative upper flap setting ($\delta_u = -30°$) allowed higher maximum-trimmed lift coefficients to be attained.

The landing gear had a large effect on the trimmed results (fig. 11(c)). With the landing gear down there was a large increase in drag coefficient which caused a large reduction in L/D. For example, with an upper flap setting of -20° and a lift coefficient of 0.3, the drag coefficient was increased by over 70 percent reducing the L/D from 4 to 2.3. In addition, the presence of the landing gear required a large reduction in lower flap setting to maintain lift coefficient (about 10°

with $\delta_u = -20°$ and $C_L = 0.3$), indicating that the nose-down pitching moment caused by the landing gear was large. (The reduction in trim drag due to the decrease in lower flap deflection was negligible.)

Lateral-Directional Aerodynamic Characteristics

With sideslip or lateral-directional control deflection an abrupt change in the yawing-moment coefficient and rolling-moment coefficient occurred at angles of attack near 20° (See, e.g., figs. 12(a) and 13(a).). In some cases, the coefficients changed signs. Tuft studies indicated that this was due to separation of the airflow on the upstream-outboard fin very similar to that which occurred on the HL-10 aircraft (ref. 3). Examination of the data indicates that the angle of attack at which separation occurred was sensitive to anything that affected the aerodynamic loading of the fin. In every case this angle of attack was larger than that at maximum L/D; thus separation would probably not occur during normal trimmed flight but might occur during maneuvering flight.

The following significant features concerning the lateral-directional control data should be noted. The yawing moment produced by the upper rudders (fig. 13) was accompanied by adverse rolling moment ($C_{l_{\delta_r}}/C_{n_{\delta_r}} \approx -(1/2)$) that was about the same level as for the M2-F2 and HL-10 aircraft. Comparison of the data in figure 14 with figure 13 shows that the yawing moment produced by the lower rudders is accompanied by less adverse rolling moment at low angles of attack, but that this yawing moment varies more with angle of attack. At angles of attack below about 15° the rolling moment produced by both the upper and lower flap systems was accompanied by very little yawing moment (figs. 15 and 16). The lower flaps are only about one fourth as effective as the upper flaps for controlling roll.

The effect of sideslip on the control effectiveness of the differential upper flaps, differential lower flaps, and upper rudders was examined at sideslip angles up to 6°, but was found to be insignificant; hence the data are not presented.

CONCLUDING REMARKS

With the landing gear up the maximum L/D achieved was 5.2 untrimmed and 4.4 trimmed. At the trimmed L/D of 4.4, the control settings required did not provide a margin for maneuvering. A usable value would probably range from about 3-1/2 to 4, which is slightly higher than that for the M2-F2 and HL-10 lifting body aircraft.

Lowering the landing gear caused a large nose-down pitching-moment increment and a large increase in drag, and consequently, a large reduction in L/D. At an upper flap setting of -20° and a C_L of 0.3 the lower flap setting would have to be reduced about 10° to trim the aircraft and maintain C_L. For these conditions the L/D would be reduced by 1.7 because of the drag increase.

Longitudinal results for one control setting were compared with those obtained from testing the 1/5 scale wind-tunnel model of reference 4. Very good agreement was shown.

With sideslip or lateral-directional control deflection, separation of the airflow on the upstream-outboard fin occurred at angles of attack near 20°. This separation was very similar to that which occurred on the HL-10 aircraft. Abrupt changes in the lateral-directional data occurred with this separation; however, the angle of attack at which separation occurred was larger than that at maximum L/D. Thus, separation would probably not occur during normal trimmed flight but might occur during maneuvering flight.

Ames Research Center
National Aeronautics and Space Administration
Moffett Field, Calif., 94035, April 8, 1970

REFERENCES

1. Pyle, Jon S., and Swanson, Robert H.: Lift and Drag Characteristics of the M2-F2 Lifting Body During Subsonic Gliding Flight. NASA TM X-1431, 1967.

2. Mort, Kenneth W.; and Gamse, Berl: Full-Scale Wind-Tunnel Investigation of the Aerodynamic Characteristics of the M2-F2 Lifting Body Flight Vehicle. NASA TM X-1588, 1968.

3. Gamse, Berl; and Mort, Kenneth W.: Full-Scale Wind-Tunnel Investigation of the HL-10 Manned Lifting Body Flight Vehicle. NASA TM X-1476, 1967.

4. Dagold, R. G.: Results of a Low Speed Investigation of 20 Percent Scale SV-5P Vehicle in University of Maryland Wind Tunnel, Tenth Series. Martin Baltimore Div. Rep. No. ER 13884, Nov. 1965.

TABLE 1.– INDEX TO FIGURES

Type of data	Purpose	δ_u, deg	δ_l, deg	δ_{rf}, deg	Landing gear	Figure
Longitudinal, basic	Effect of Reynolds number	-20	10	-9	Up	4
	Effect of longitudinal control	-5	Varied	-9	Up	5 (a)
		-10				(b)
		-15				(c)
		-20				(d)
		-25				(e)
		-30				(f)
		-5		0		6 (a)
		-10				(b)
		-15				(c)
		-20				(d)
		-25				(e)
		-30				(f)
		-10		9		7 (a)
		-20				(b)
		-30				(c)
		-5		-9	Down	8 (a)
		-10				(b)
		-20				(c)
		-30				(d)
	Effect of sideslip	-20	10	-9	Up	9 (a)
					Down	(b)
	Comparison with ref. 4	-5	0	-10	Up	10
Longitudinal, trimmed	Effect of upper flaps	Varied	Varied	-9	Up	11 (a)
	Effect of rudder flare	-20,-30		-9,0,9	Up	(b)
	Effect of landing gear	-20,-30		-9	Up & Down	(c)
Lateral-directional	Effect of sideslip	-5,-20	0,20	-9	Up	12 (a)
		-20	10	-9,0,9	Up	(b)
		-20	10,20	-9	Down	(c)
	Effect of upper rudders	-20,-30	20,10	-9,9	Up	13 (a)
		-20,-30	10	-9	Up	(b)
		-20,-30	10	-9	Down	(c)
	Effect of lower rudders	-20,-30	20	0	Down	14
	Effect of differential upper flaps	-20,-30	10	-9	Up	15 (a)
		-20,-30	10	0	Up	(b)
		-20,-30	10	-9	Down	(c)
		-20	10	0	Down	(d)
	Effect of differential lower flaps	-30	20,10	-9	Up	16 (a)
		-30	10,20	-9	Down	(b)

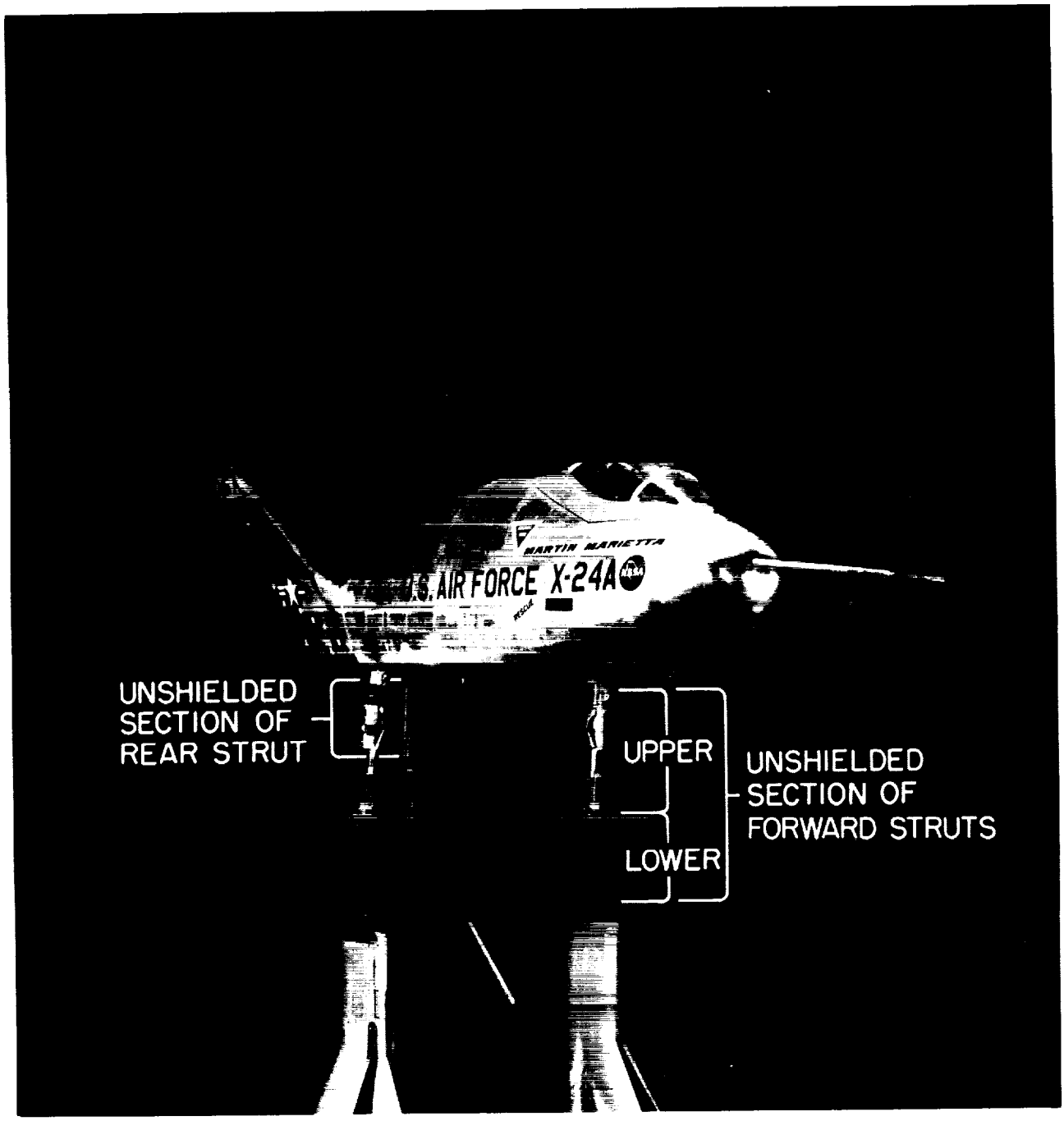

(a) Three-quarter front view.

Figure 1.- Vehicle mounted in the Ames 40- by 80-Foot Wind Tunnel.

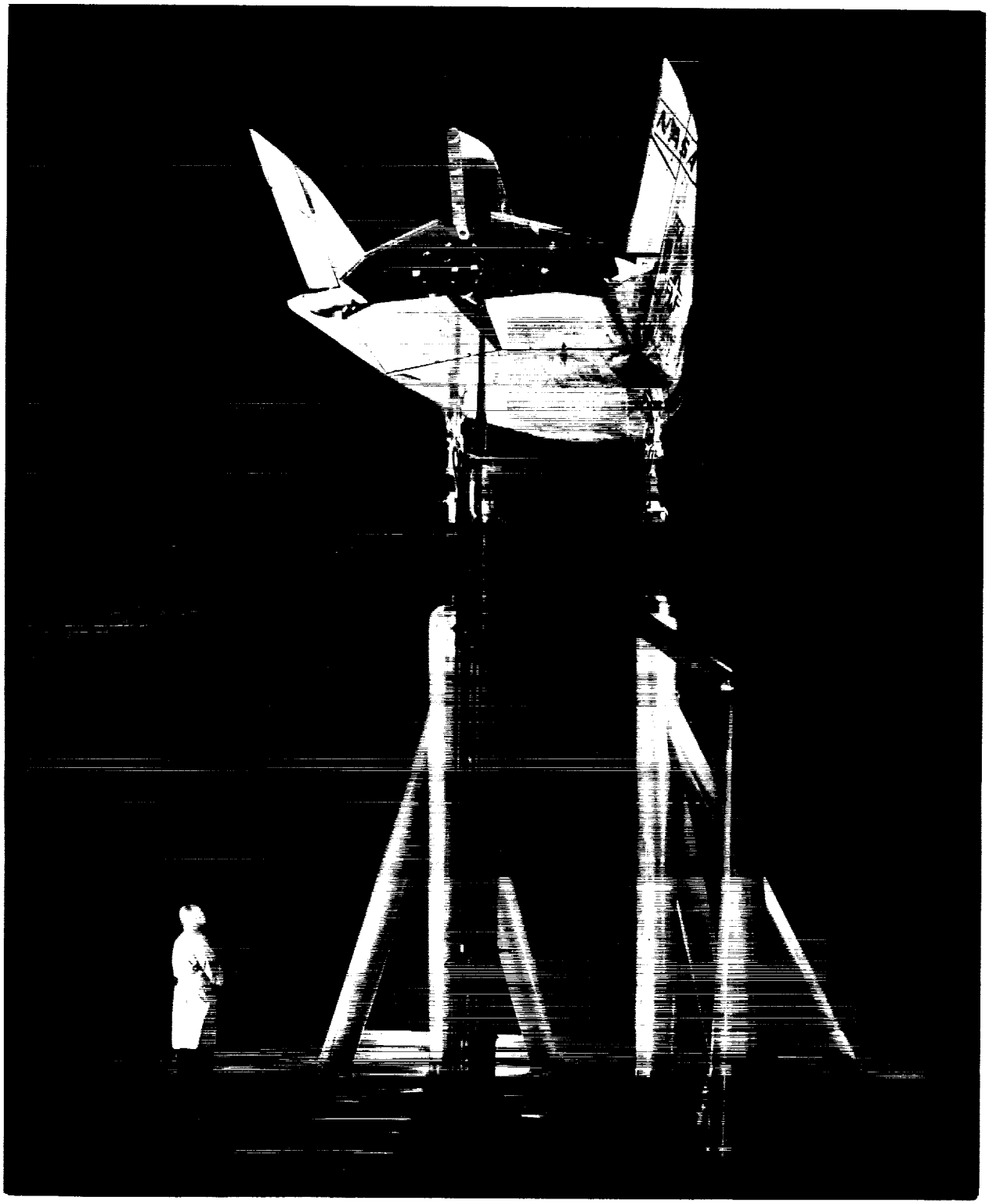

(b) Three-quarter rear view.

Figure 1.- Continued.

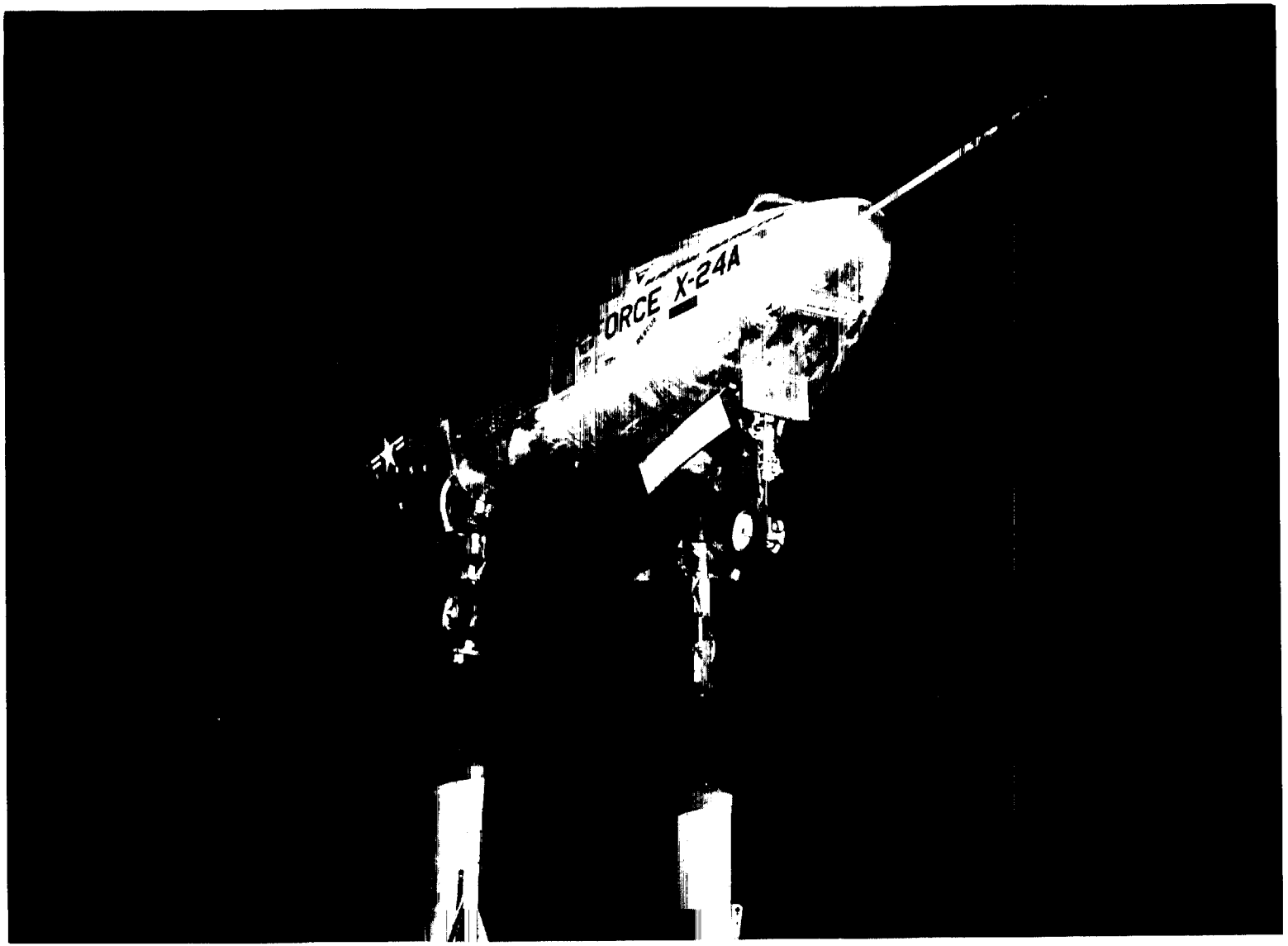

(c) Three-quarter front view with landing gear down.

Figure 1.- Continued.

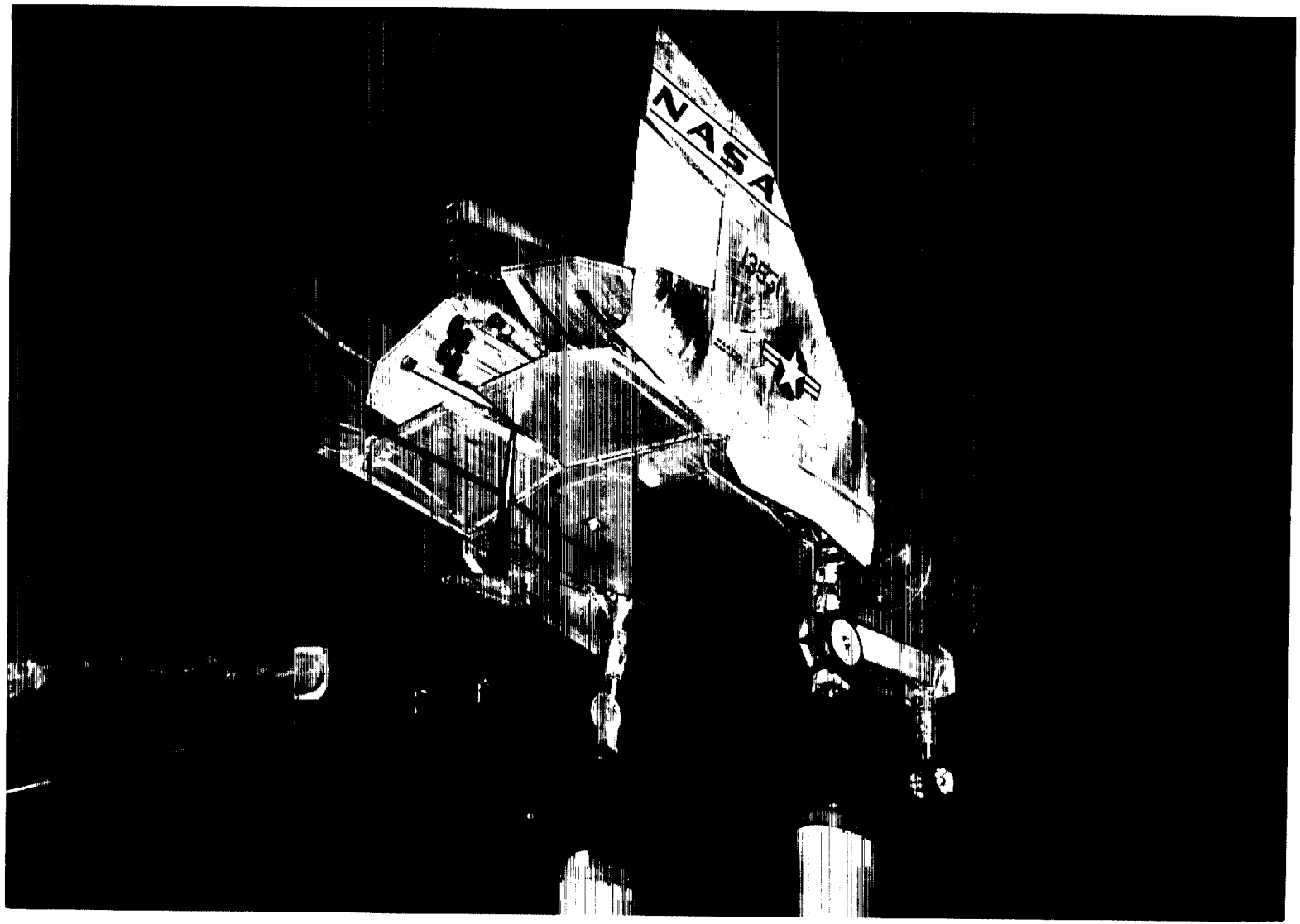

(d) Three-quarter rear view with landing gear down.

Figure 1.- Continued.

(e) Alternate mounting system.

Figure 1.- Concluded.

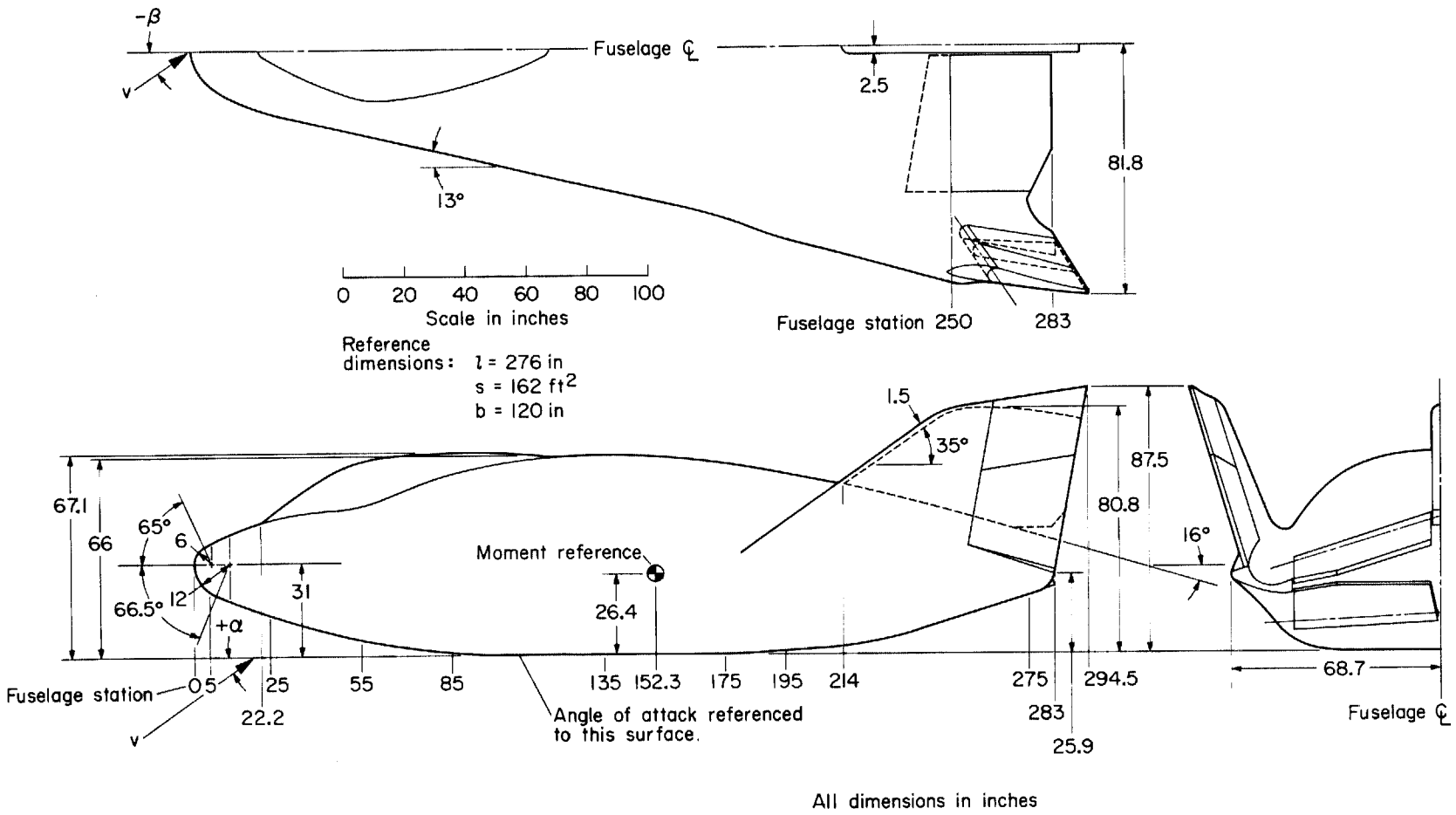

(a) Overall dimensions.

Figure 2.- Aircraft dimensions.

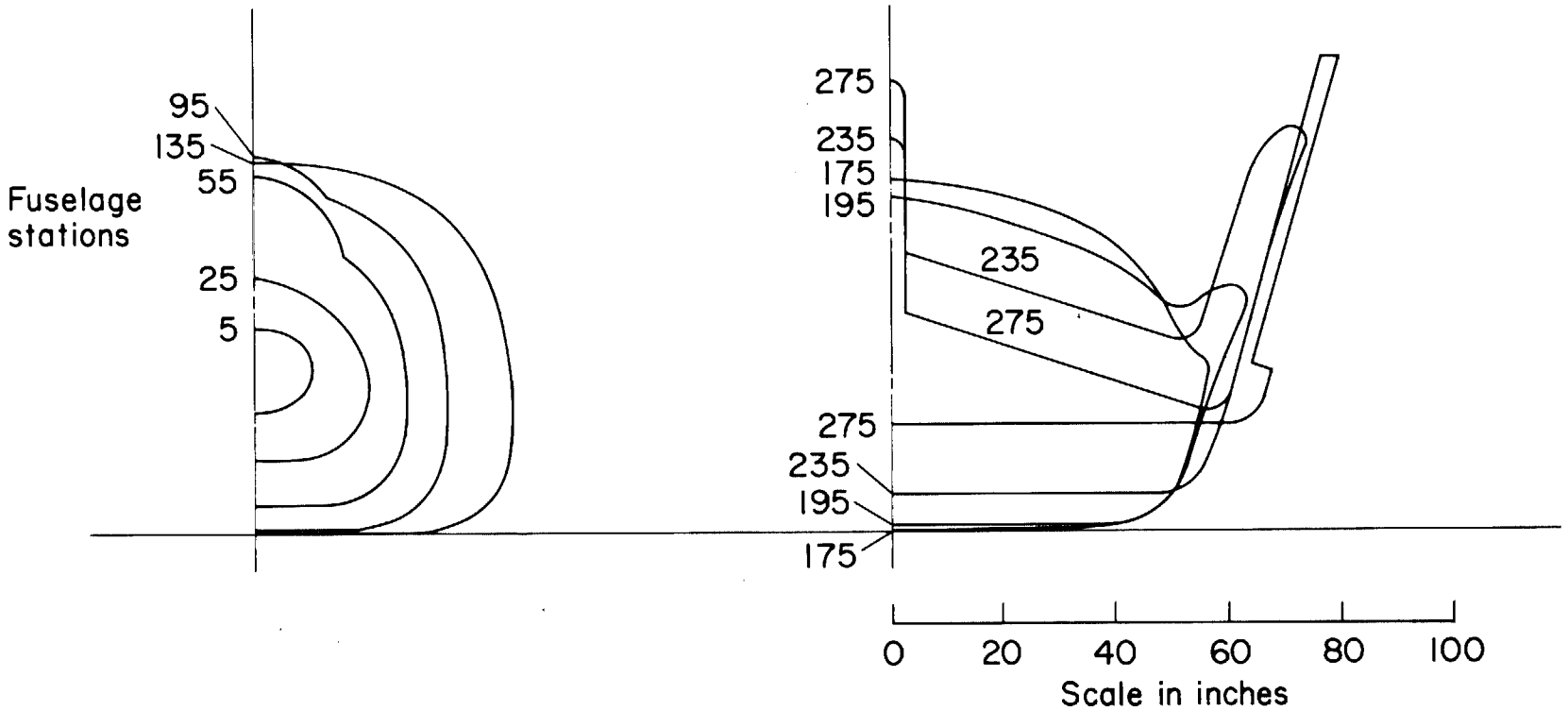

(b) Sections.

Figure 2.- Continued.

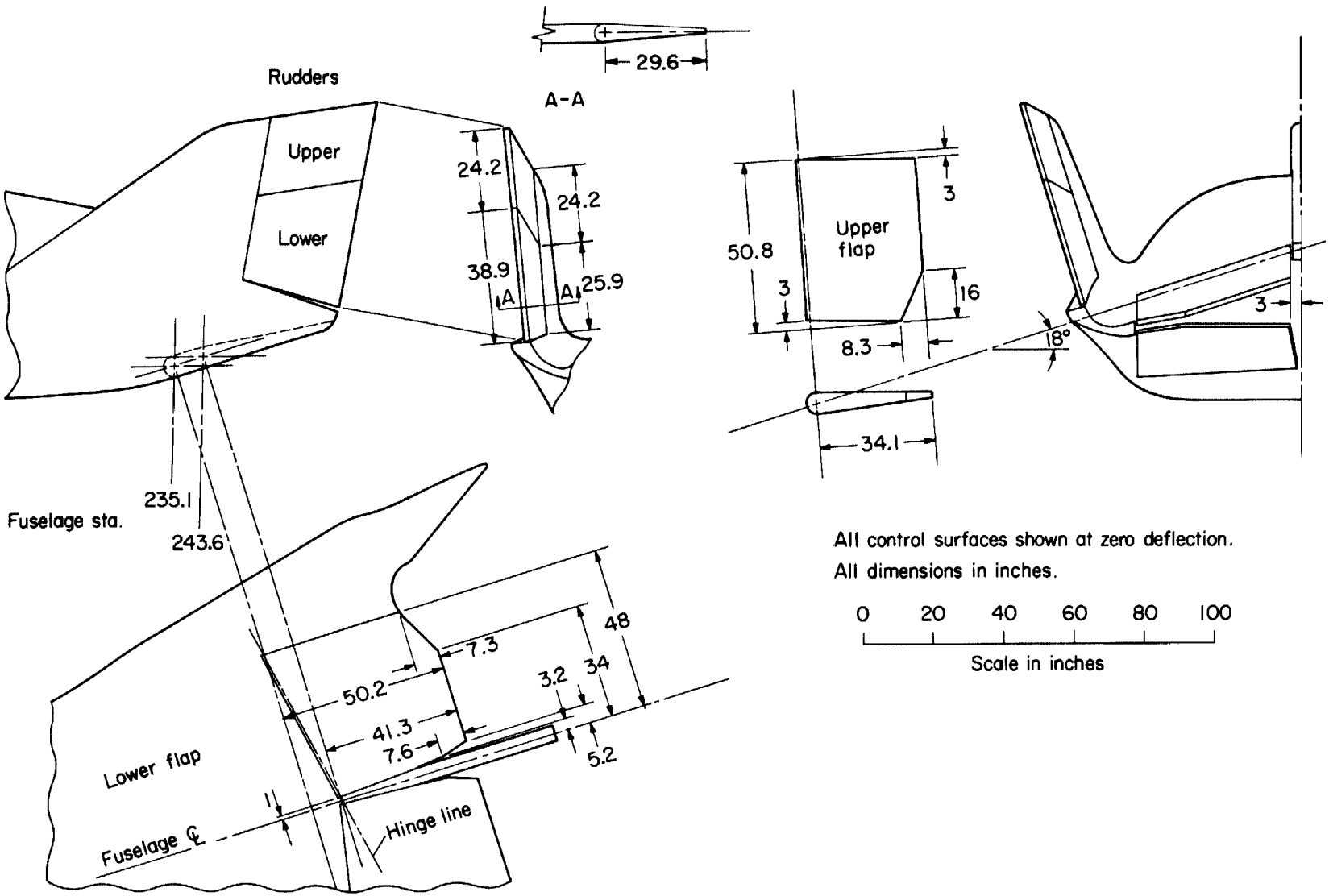

(c) Control surface detail.

Figure 2.- Concluded.

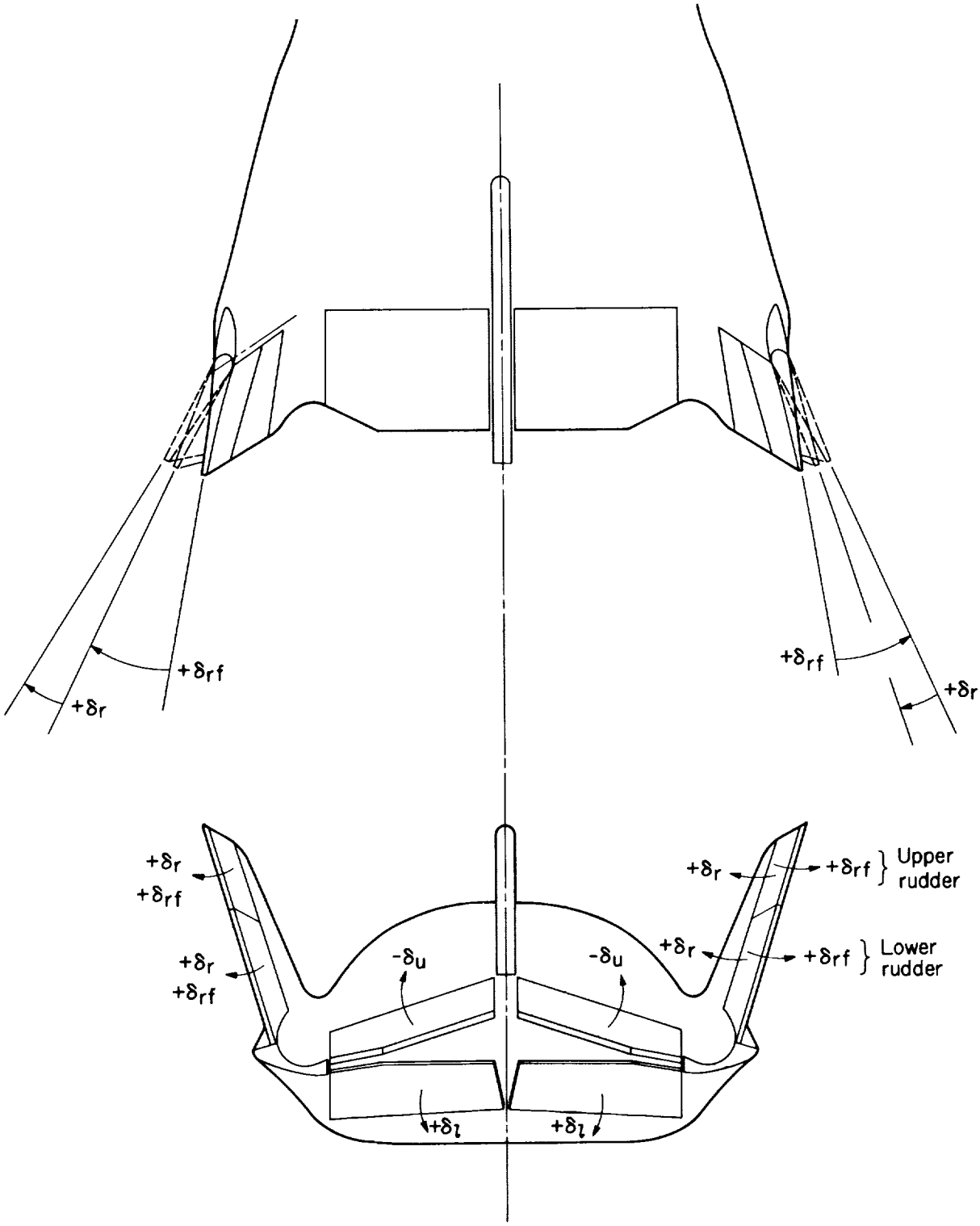

Figure 3.- Sign convention for control surface deflections.

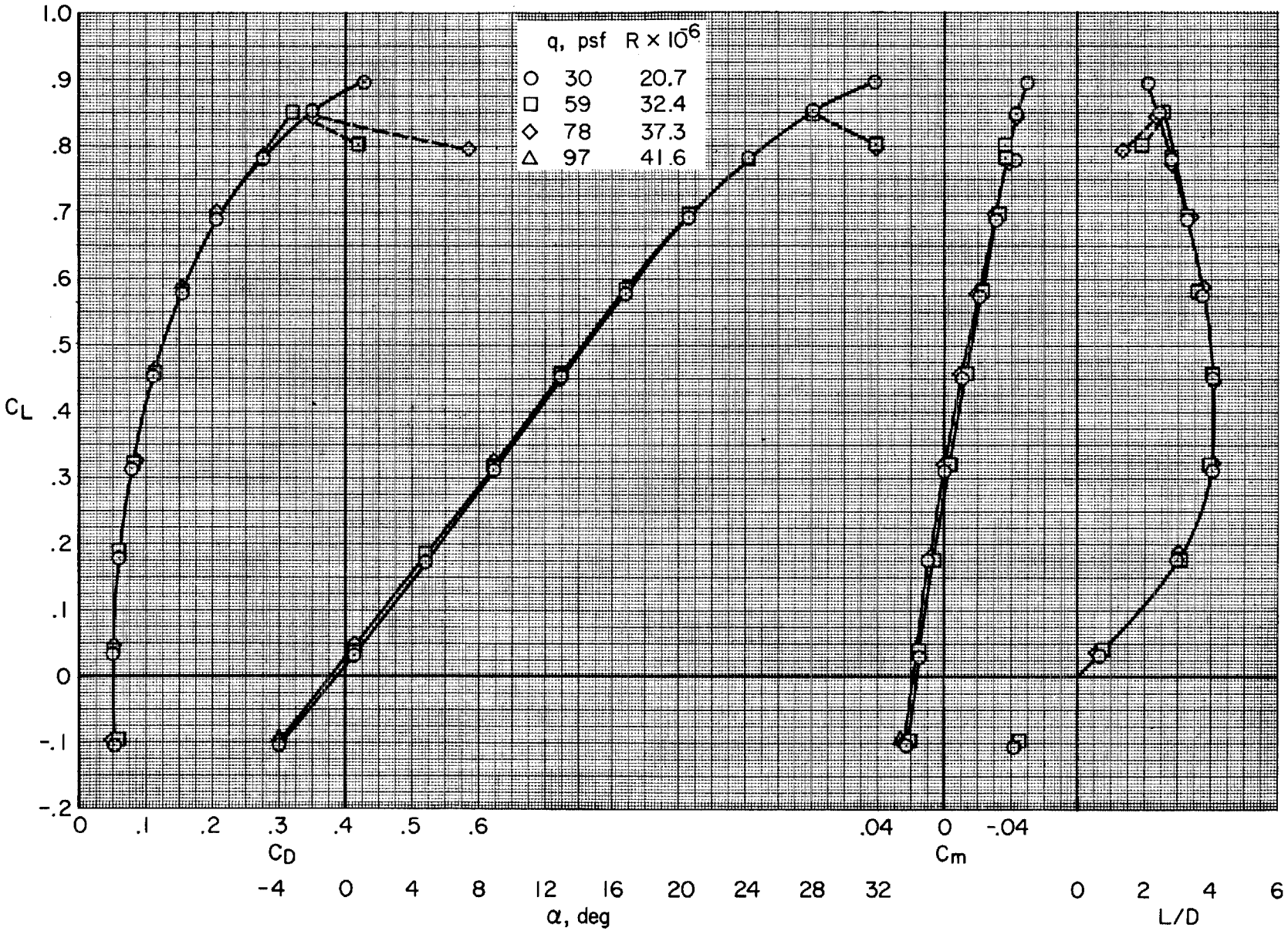

Figure 4.- Effect of Reynolds number on longitudinal aerodynamic characteristics with landing gear up; $\delta_u = -20°$, $\delta_l = 10°$, $\delta_{rf} = -9°$.

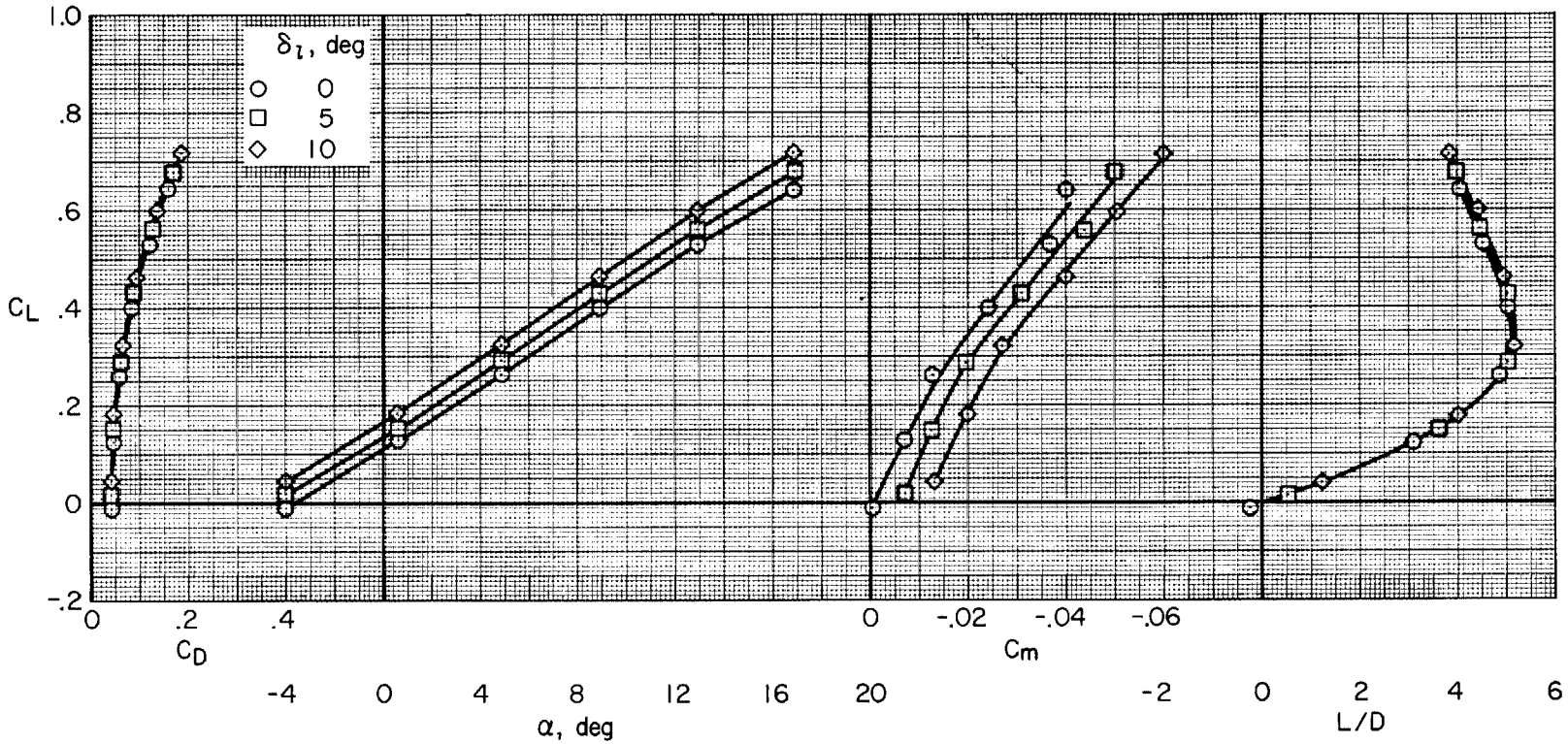

(a) $\delta_u = -5°$

Figure 5.- Longitudinal aerodynamic characteristics for several longitudinal control settings with the landing gear up and $\delta_{rf} = -9°$.

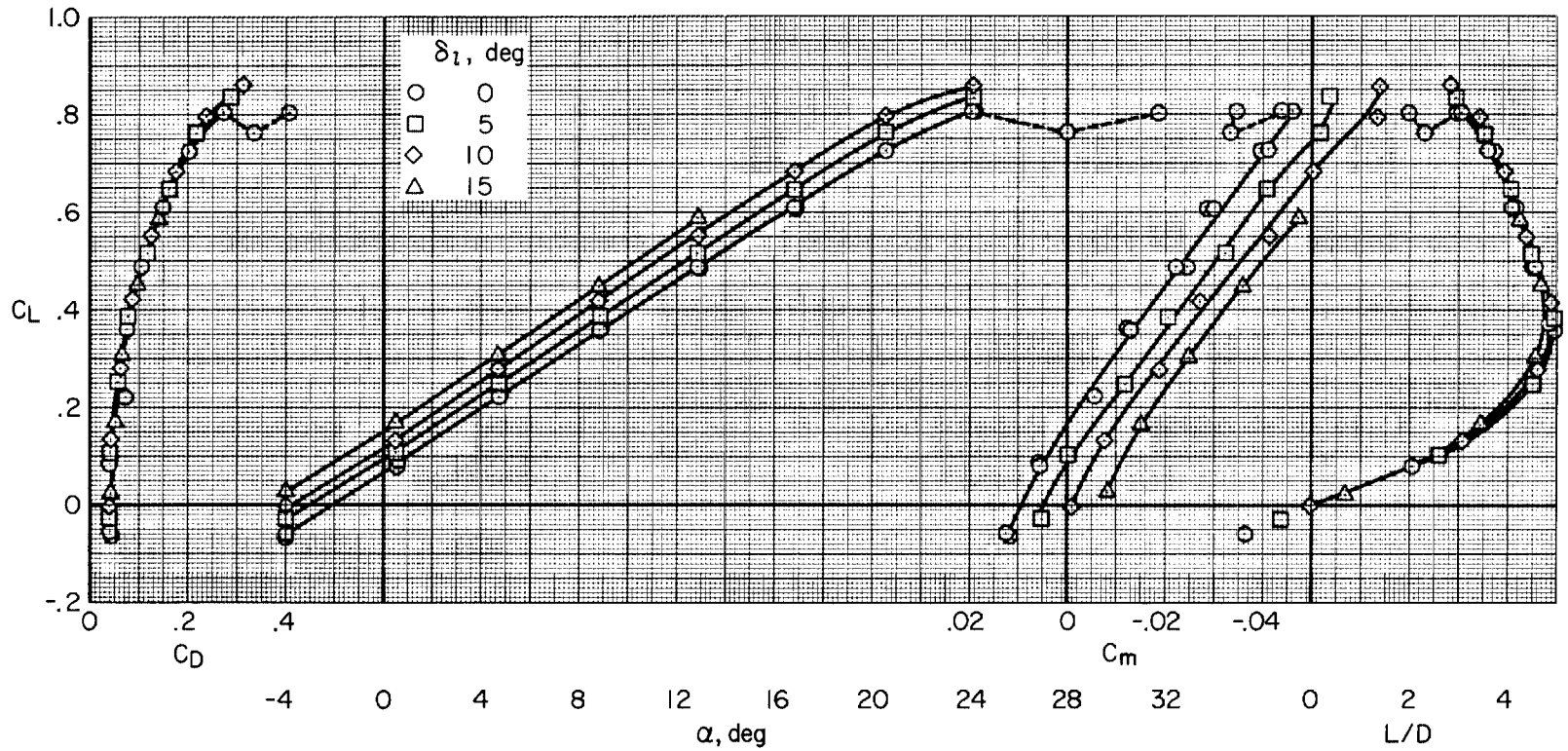

(b) $\delta_u = -10°$

Figure 5.- Continued.

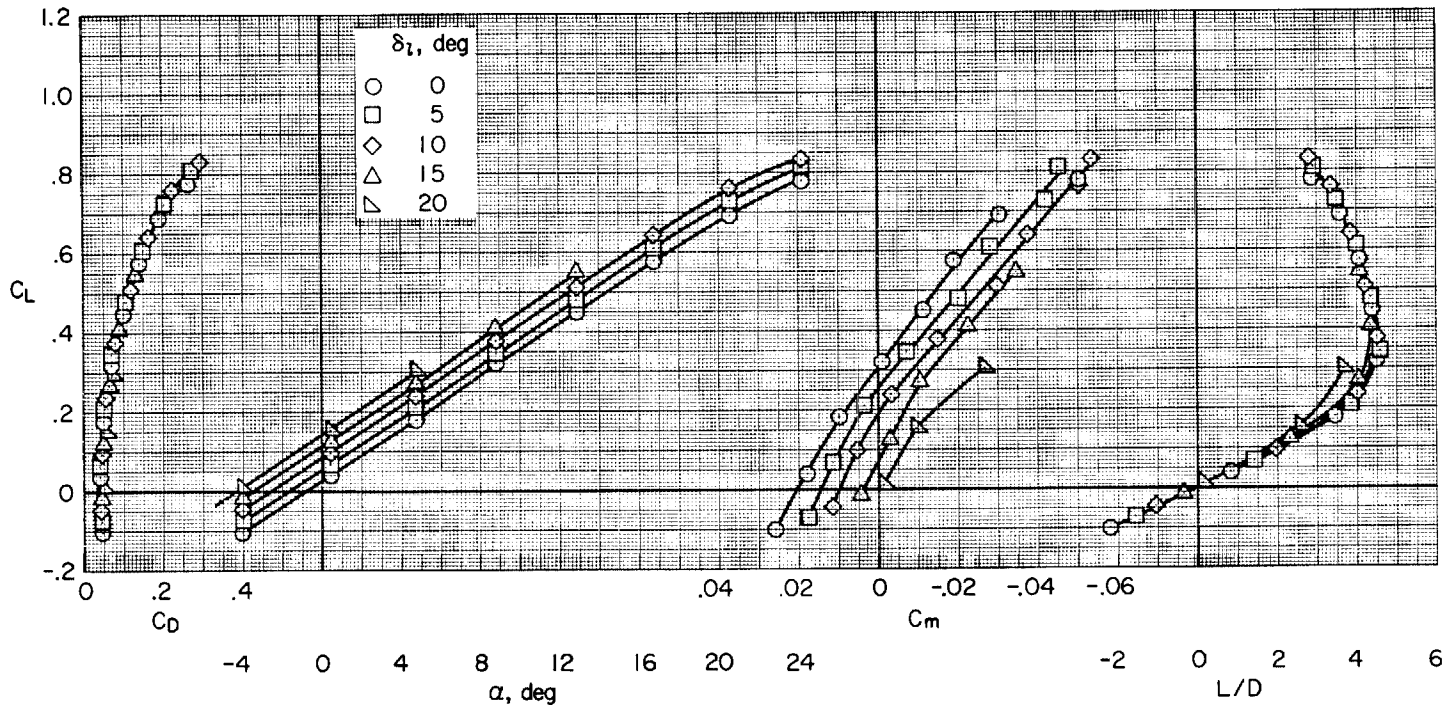

(c) $\delta_u = -15°$

Figure 5.- Continued.

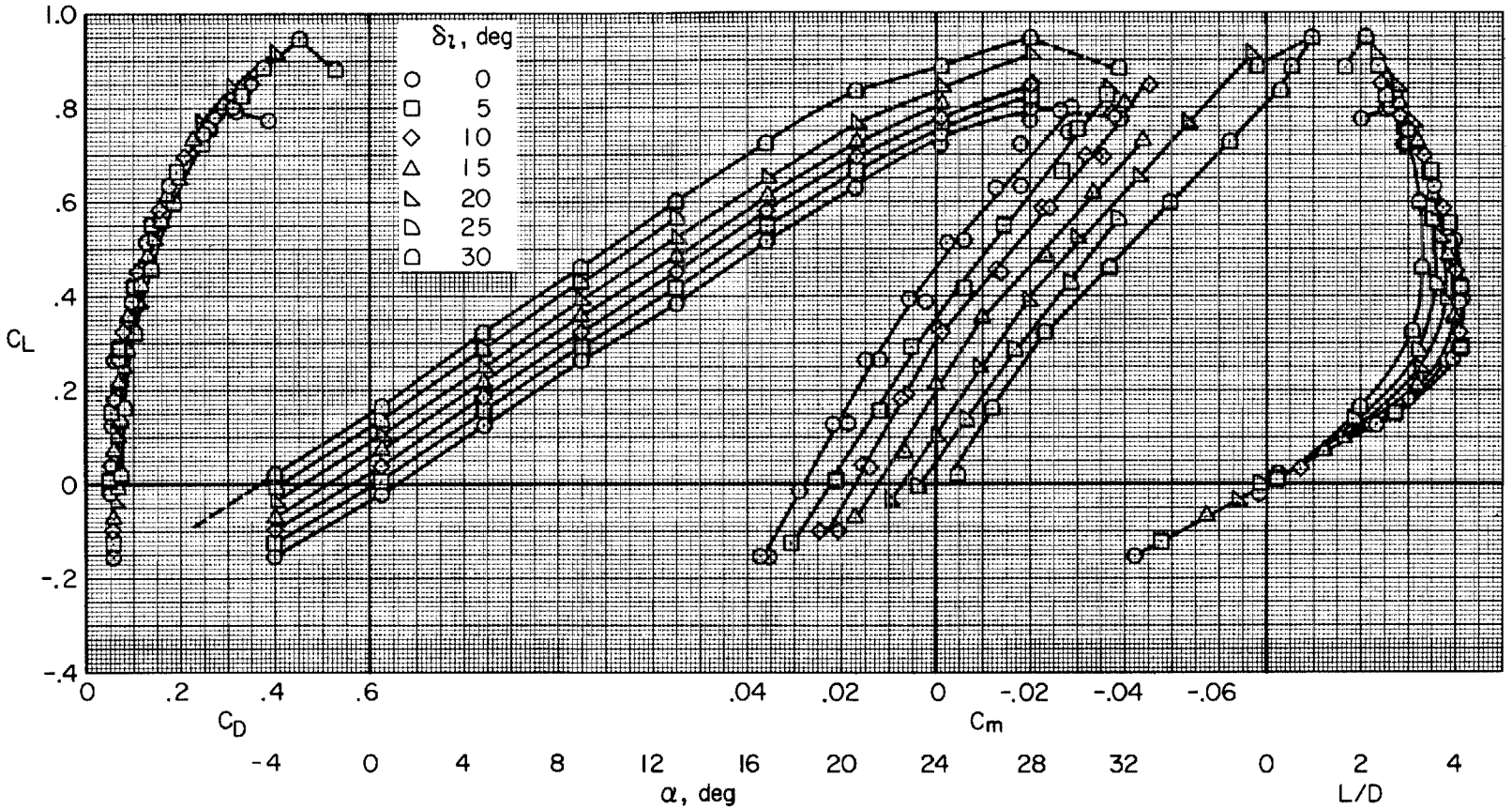

(d) $\delta_u = -20^\circ$

Figure 5.- Continued.

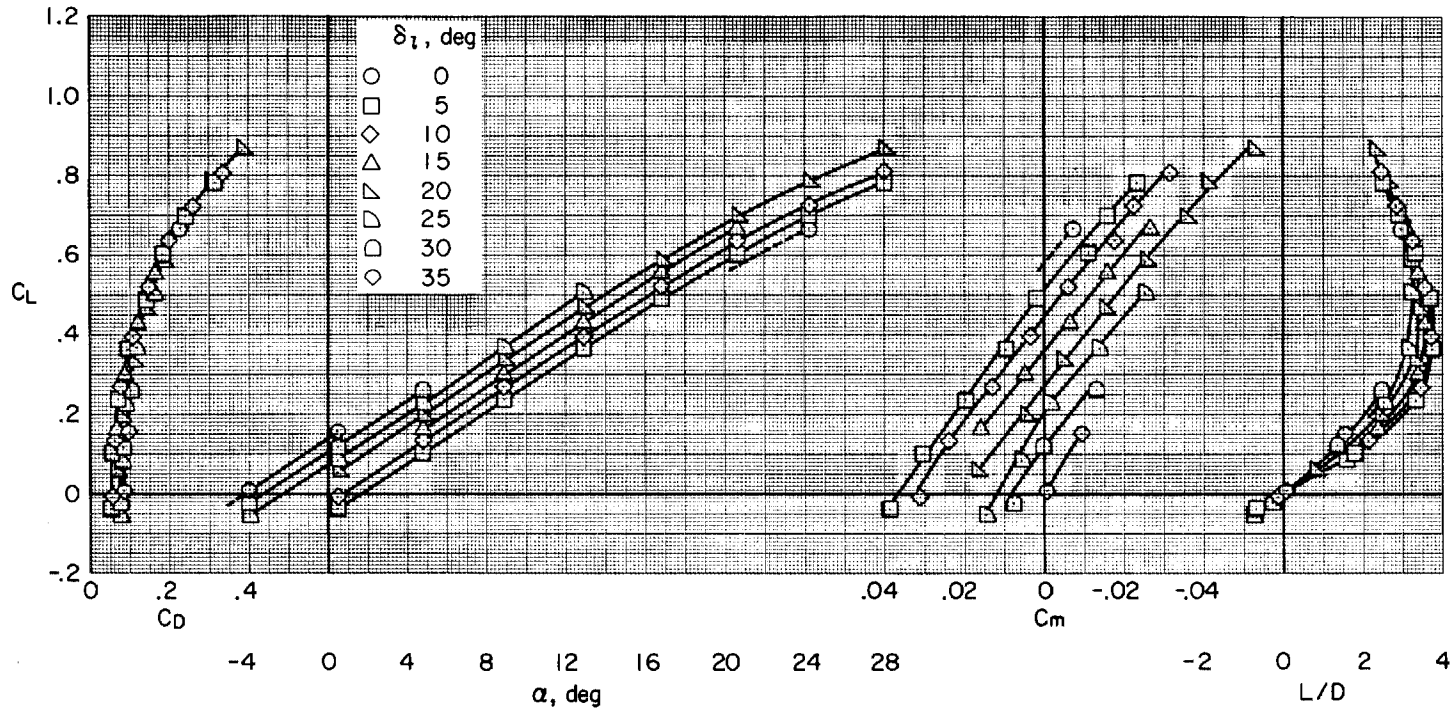

(e) $\delta_u = -25°$

Figure 5.- Continued.

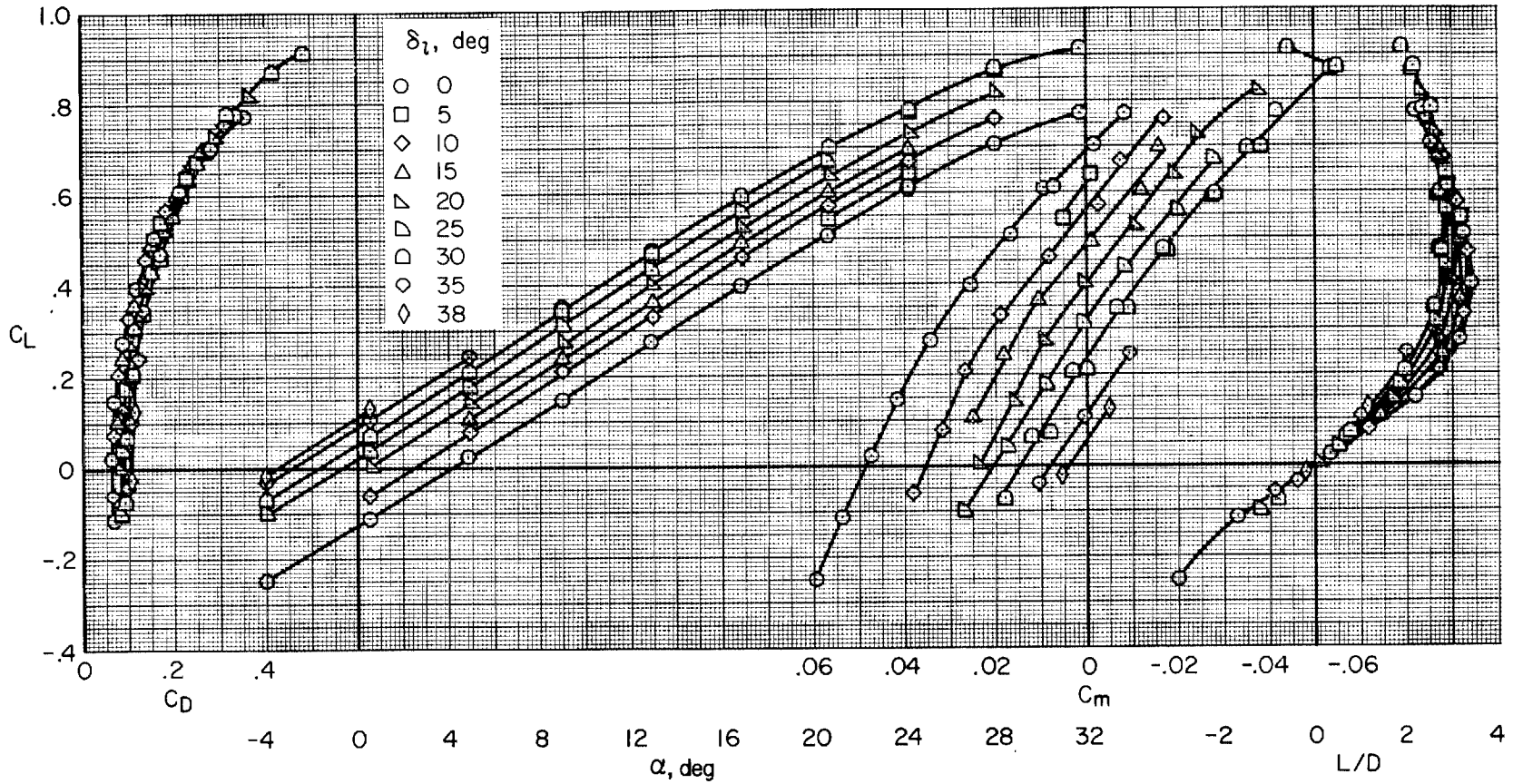

(f) $\delta_u = -30°$

Figure 5.- Concluded.

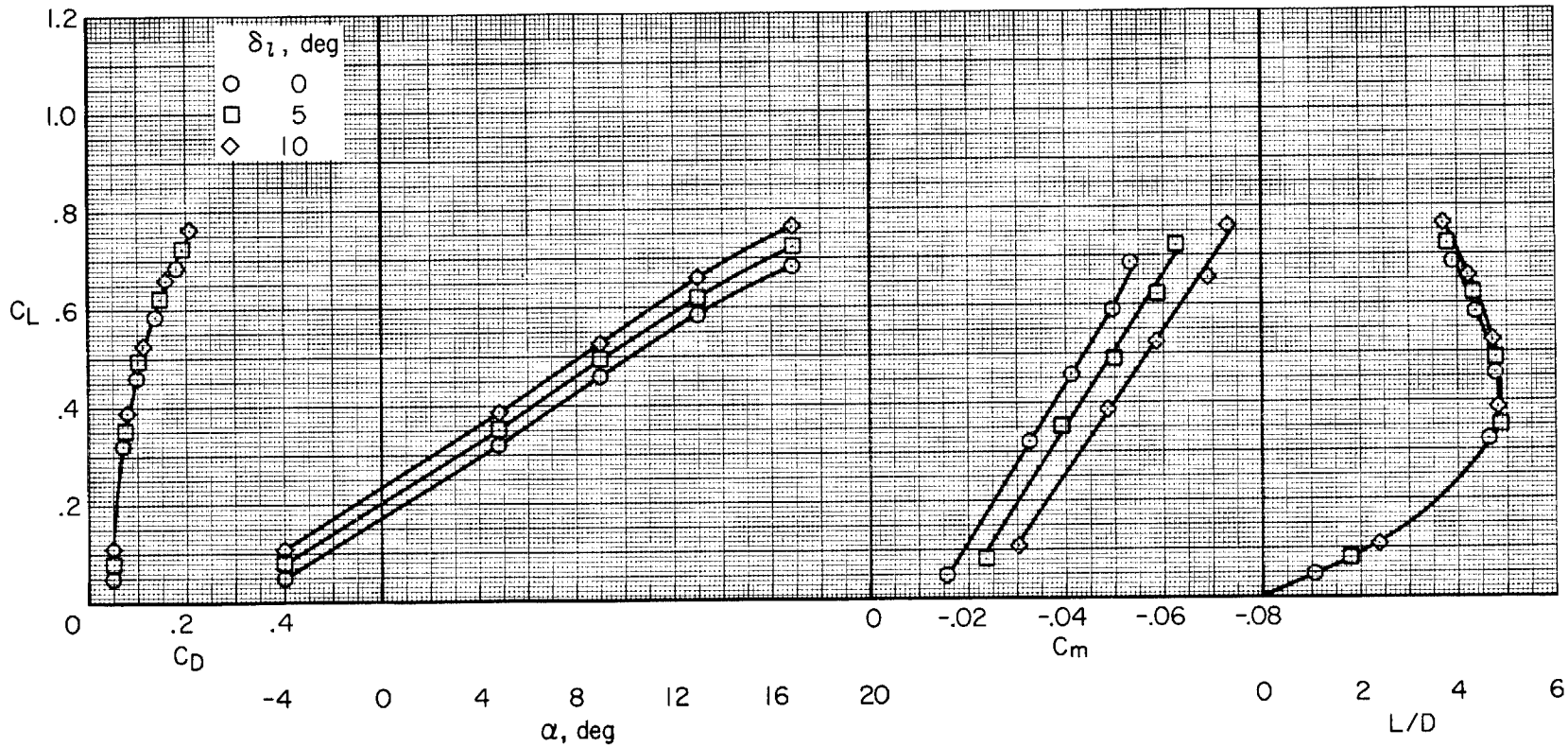

(a) $\delta_u = -5°$

Figure 6.- Longitudinal aerodynamic characteristics for several longitudinal control settings with the landing gear up and $\delta_{rf} = 0°$.

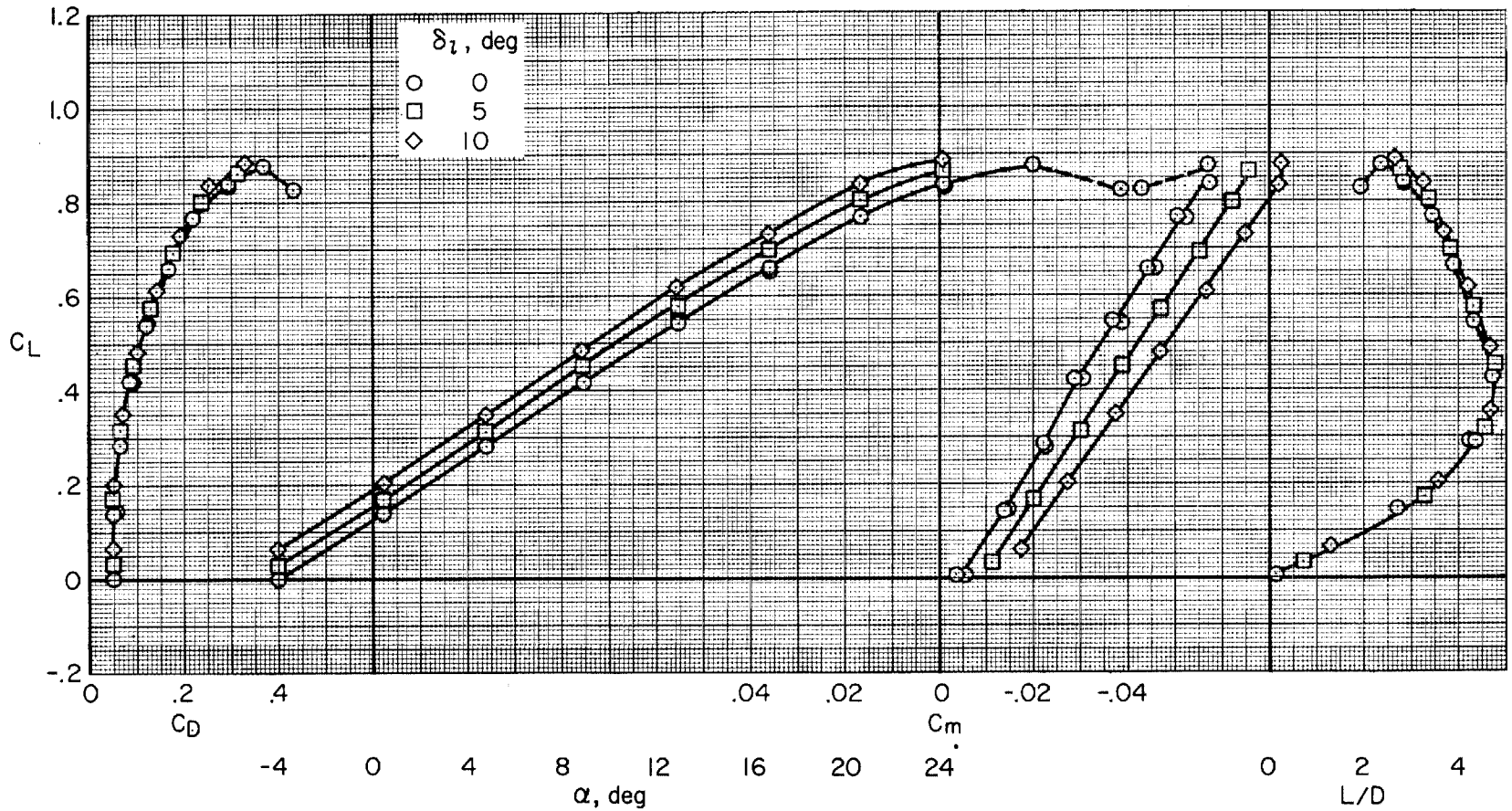

(b) $\delta_u = -10°$

Figure 6.- Continued.

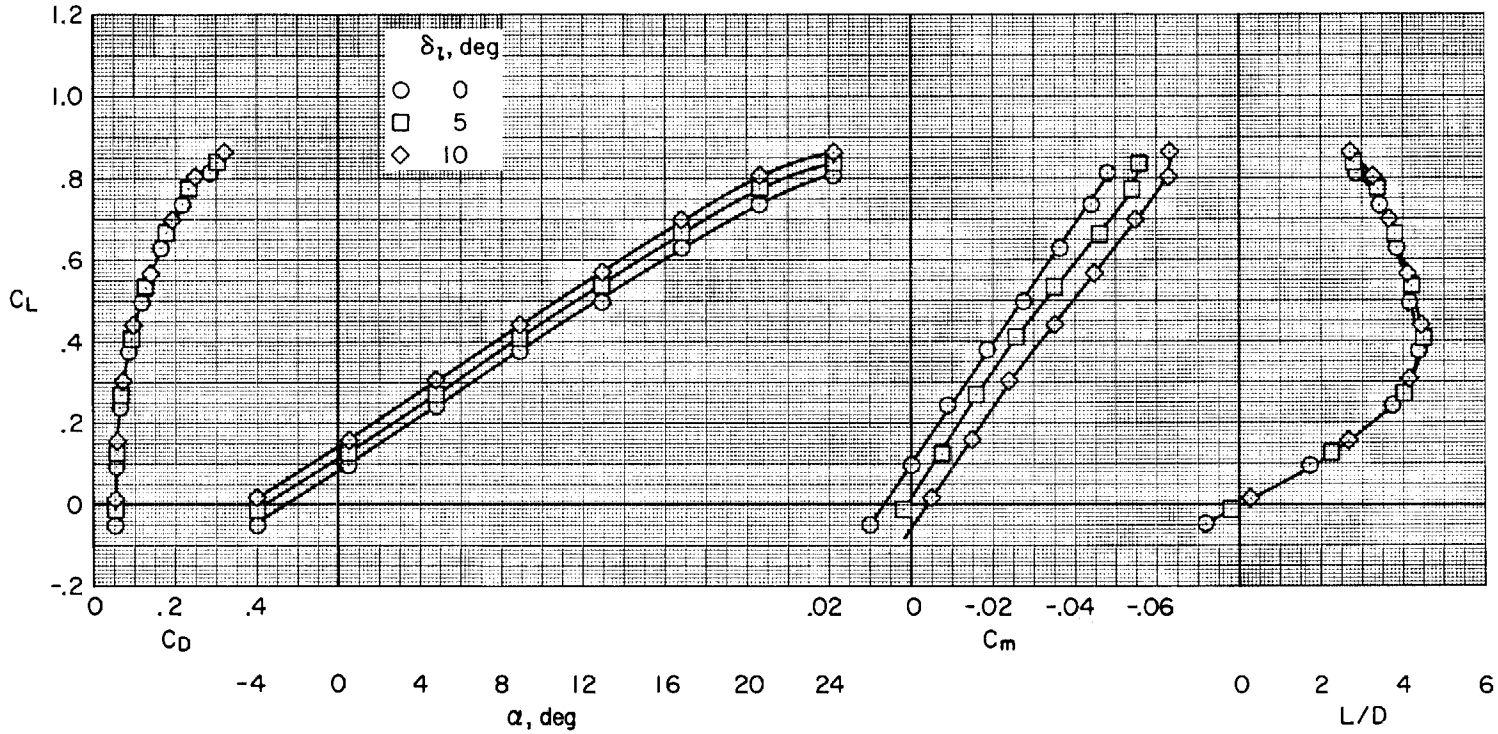

(c) $\delta_u = -15°$

Figure 6.- Continued.

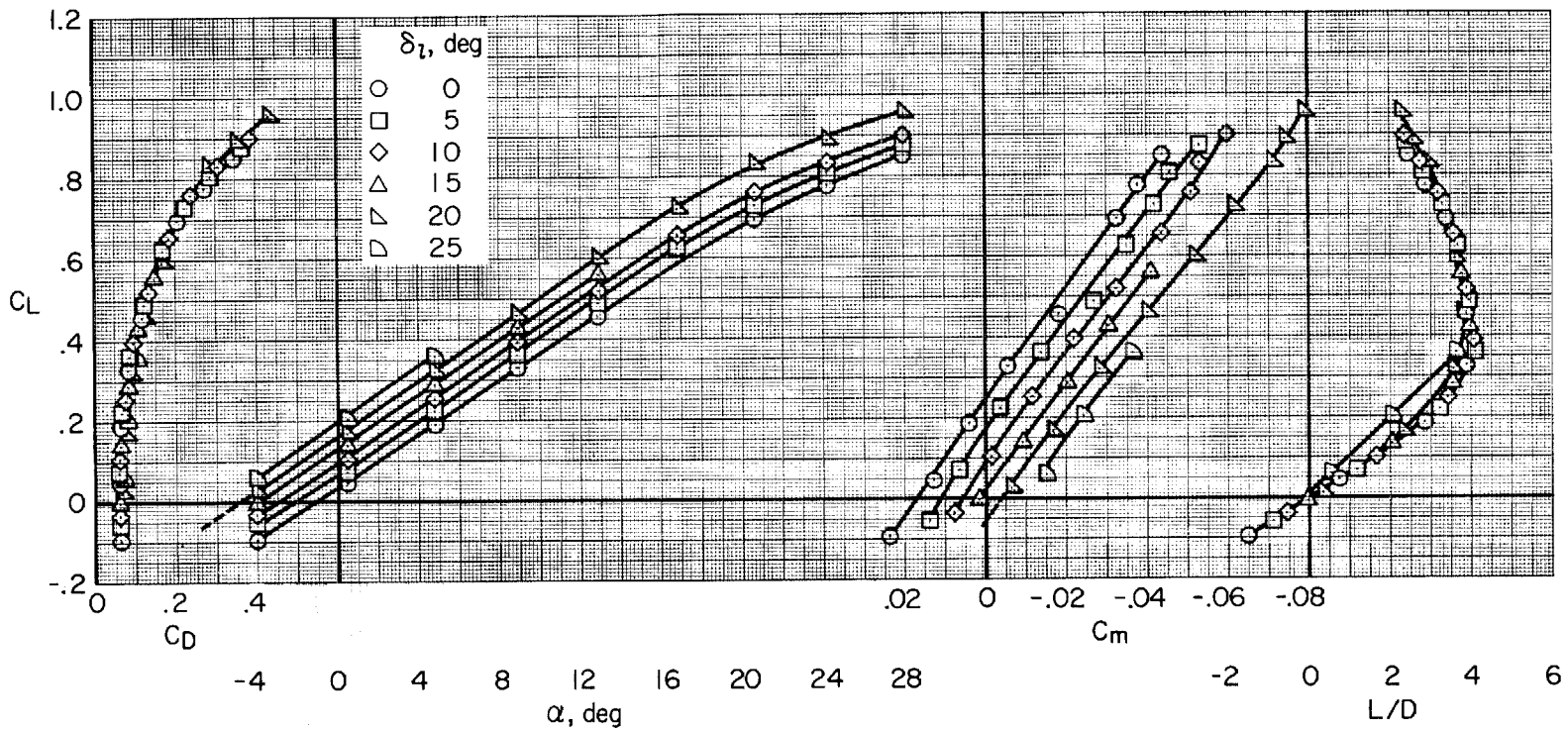

(d) $\delta_u = -20°$

Figure 6.- Continued.

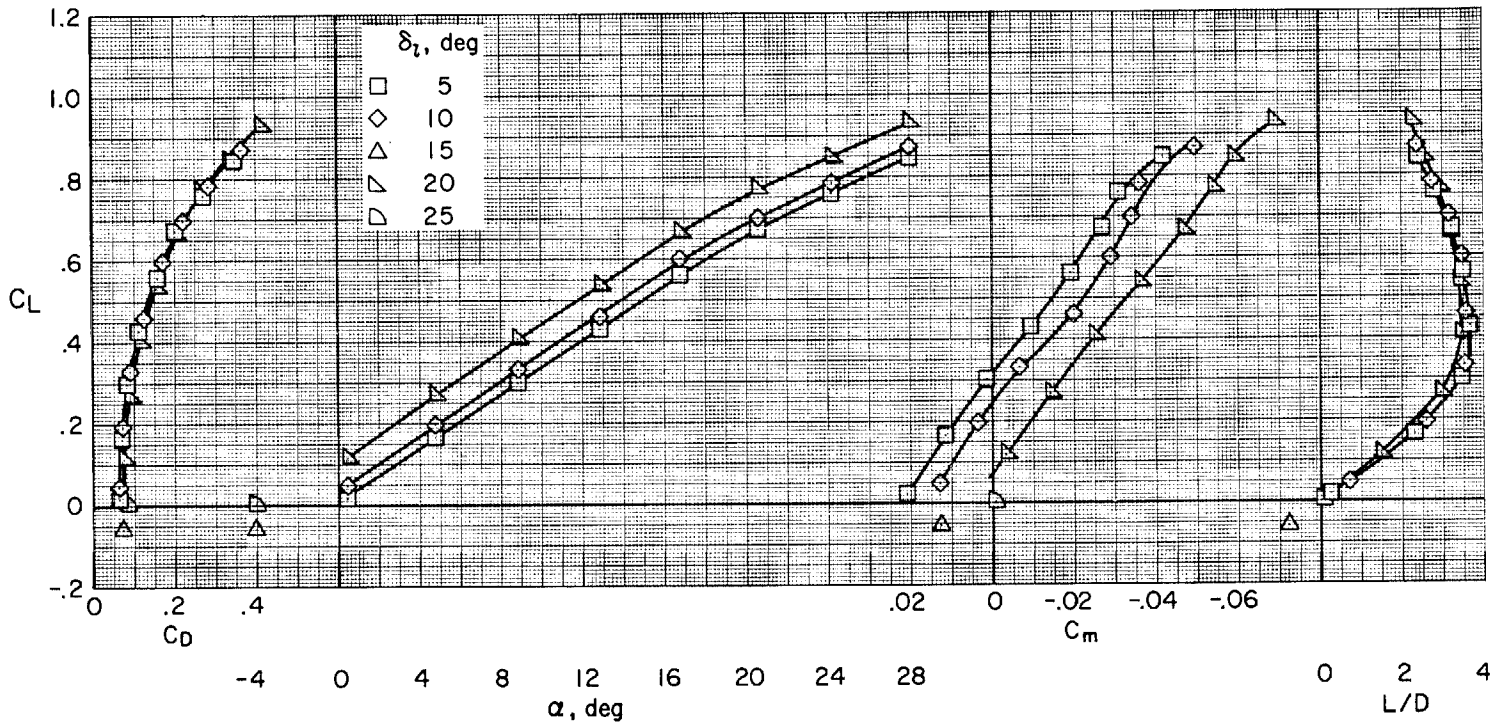

(e) $\delta_u = -25°$

Figure 6.- Continued.

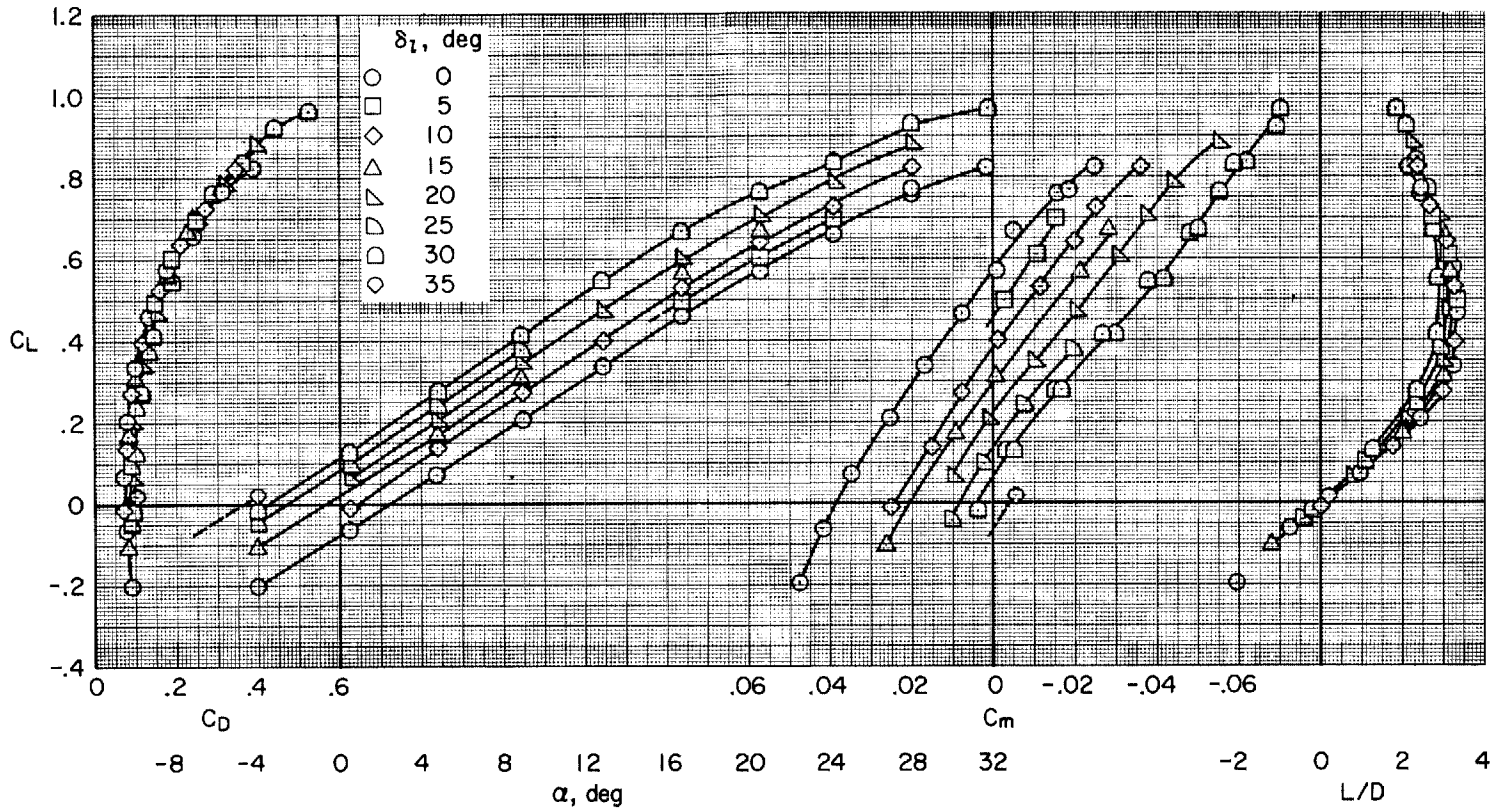

(f) $\delta_u = -30°$

Figure 6.- Concluded.

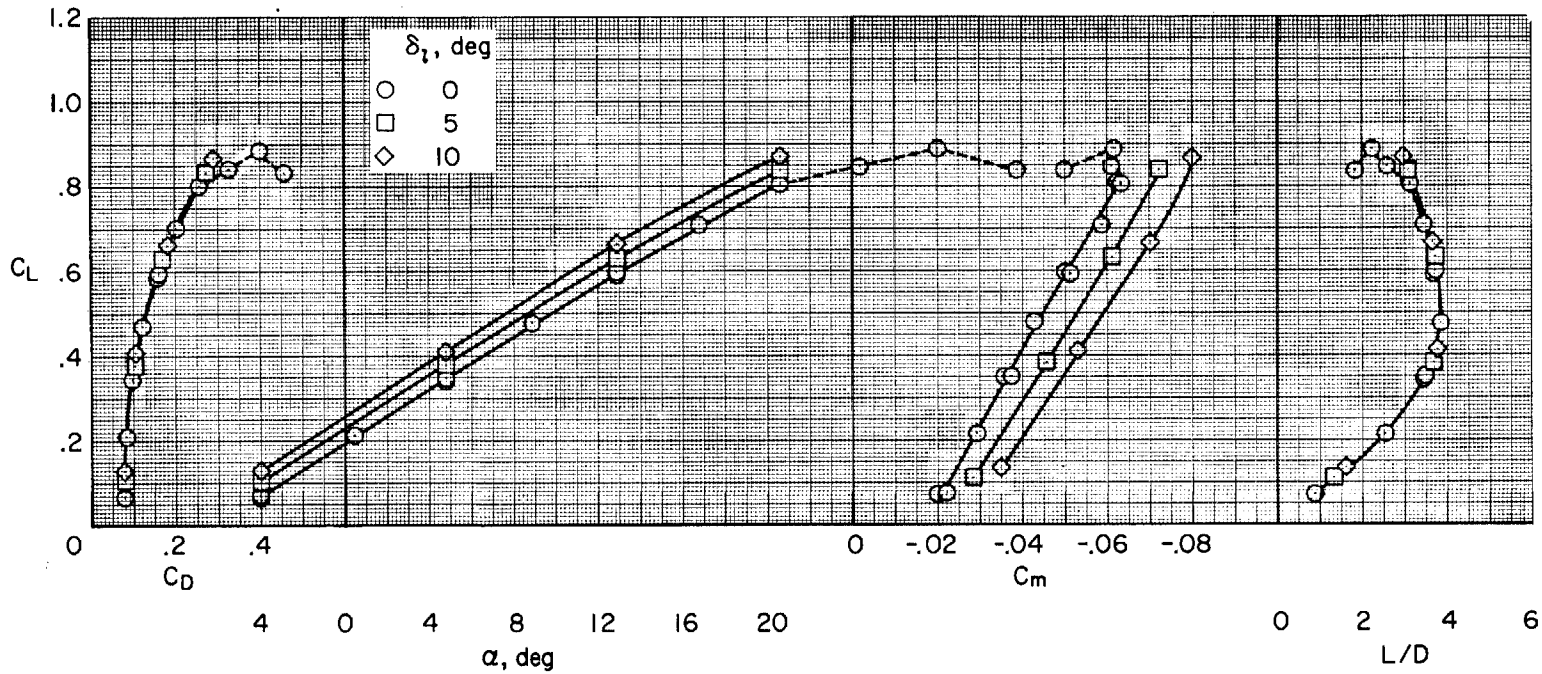

(a) $\delta_u = -10°$

Figure 7.- Longitudinal aerodynamic characteristics for several longitudinal control settings with the landing gear up and $\delta_{rf} = 9°$.

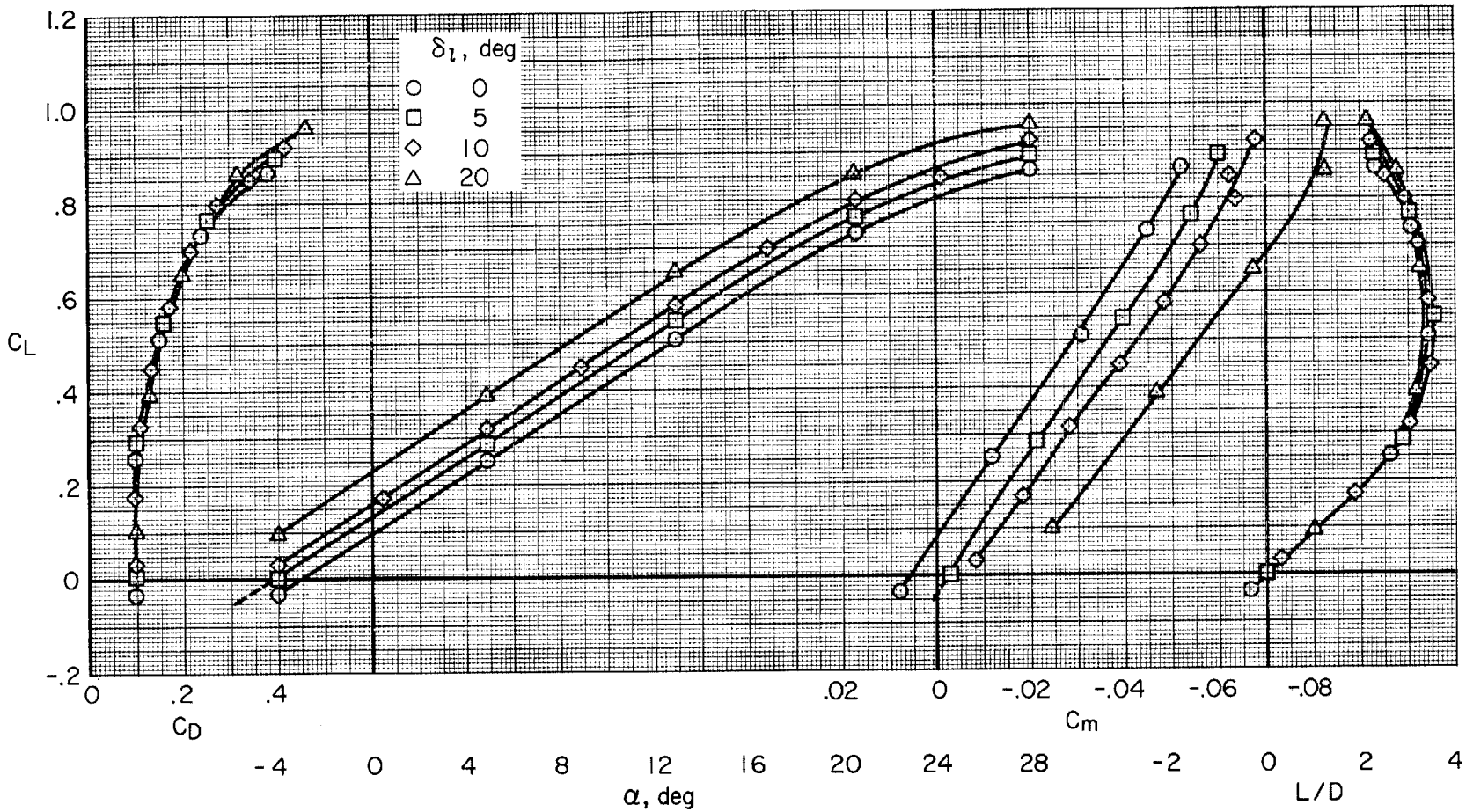

(b) $\delta_u = -20°$

Figure 7.- Continued.

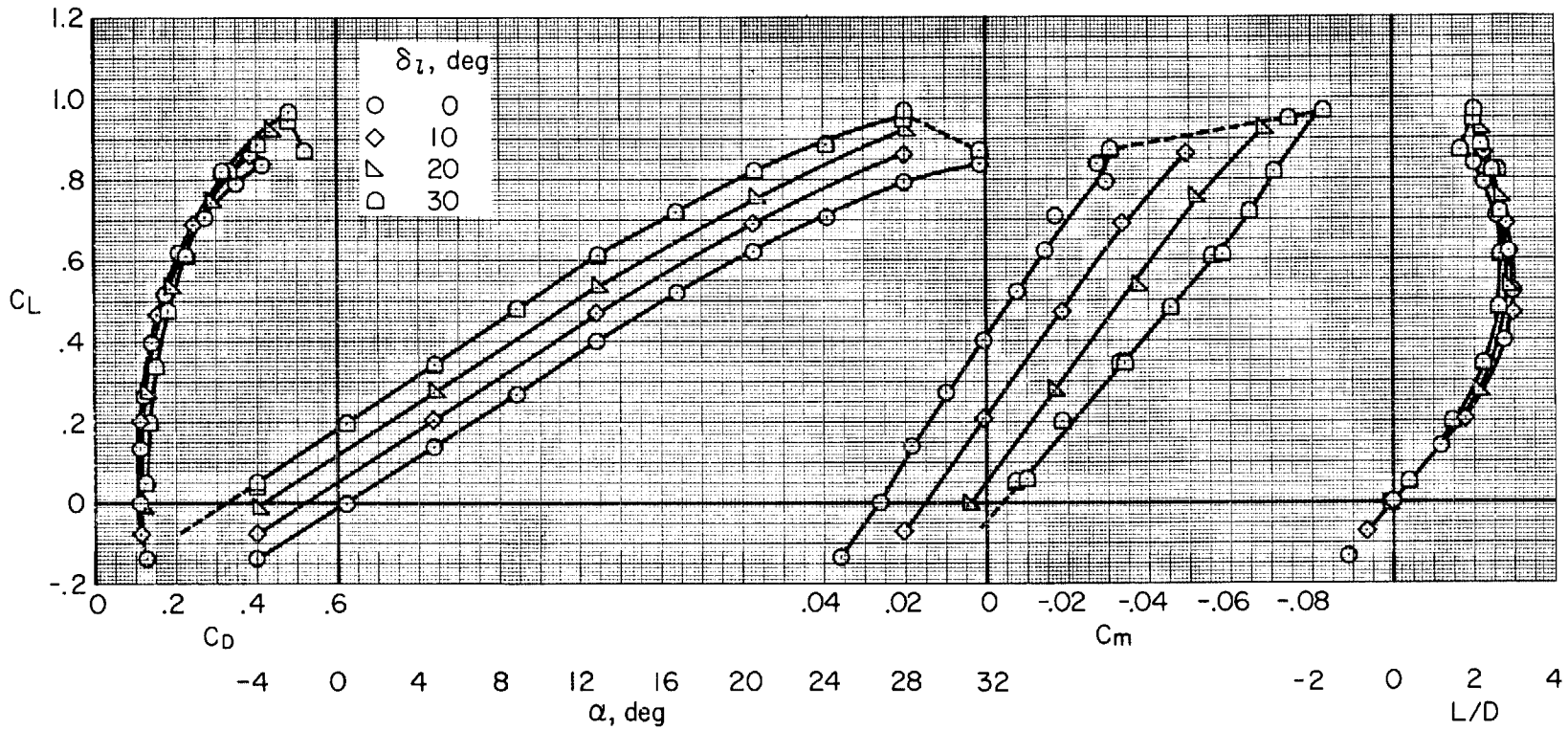

(c) $\delta_u = -30°$

Figure 7.- Concluded.

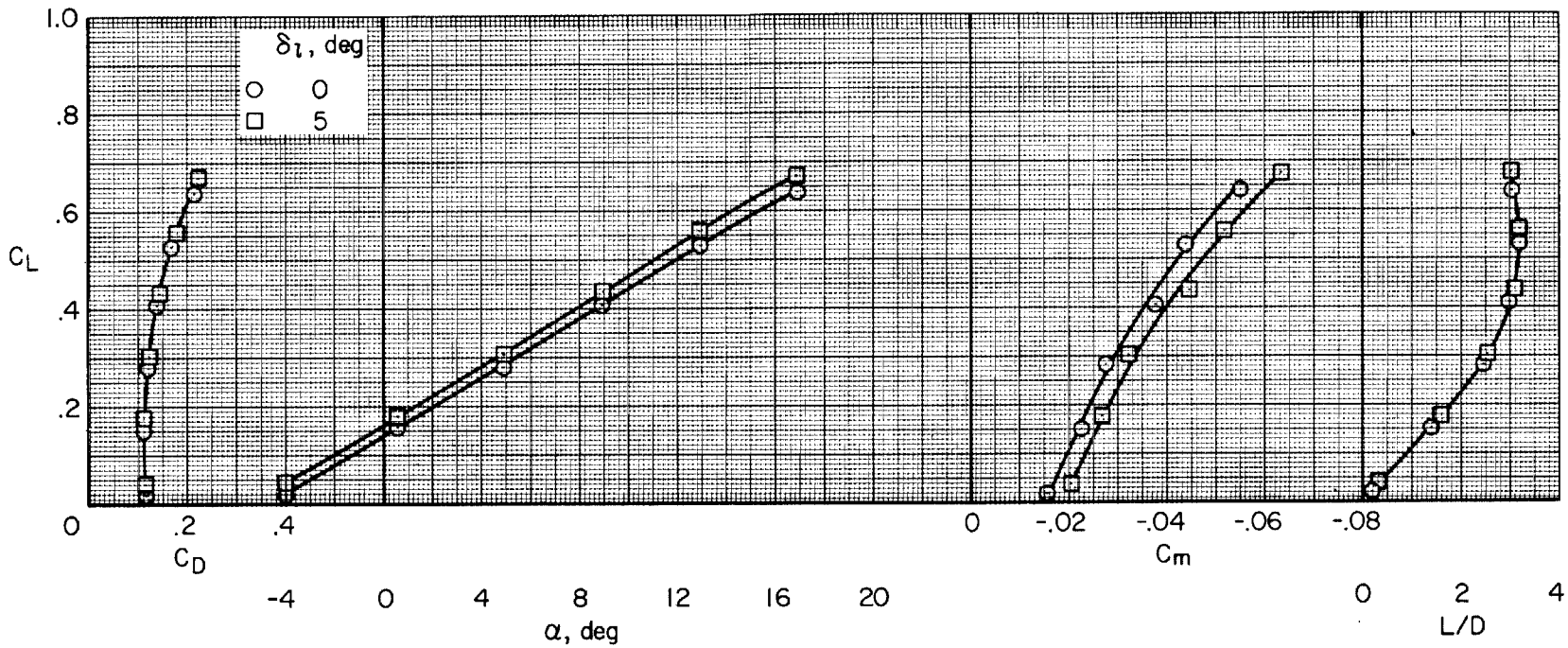

(a) $\delta_u = -5°$

Figure 8.- Longitudinal aerodynamic characteristics for several longitudinal control seetings with the landing gear down and $\delta_{rf} = -9°$.

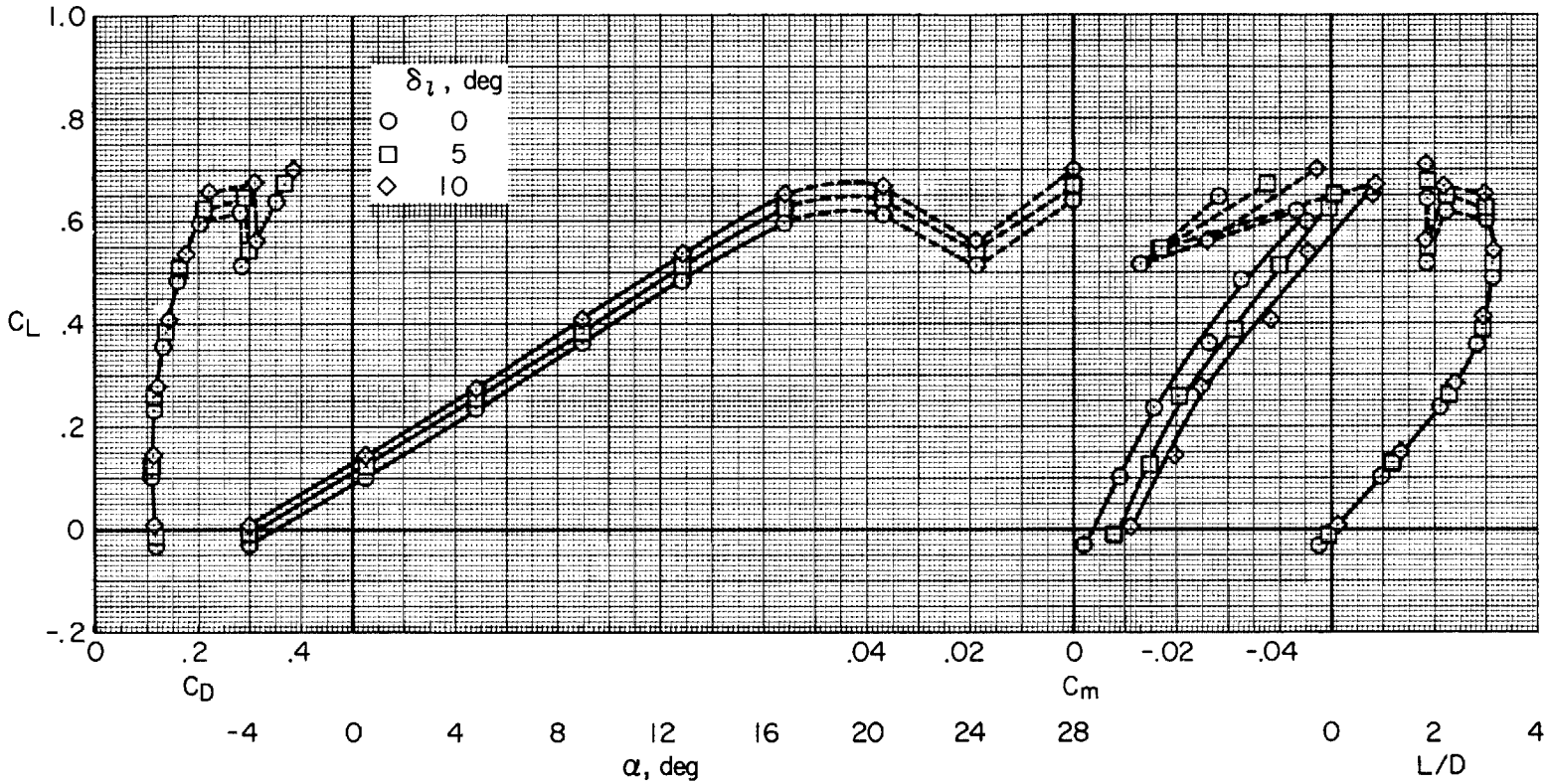

(b) $\delta_u = -10°$

Figure 8.- Continued.

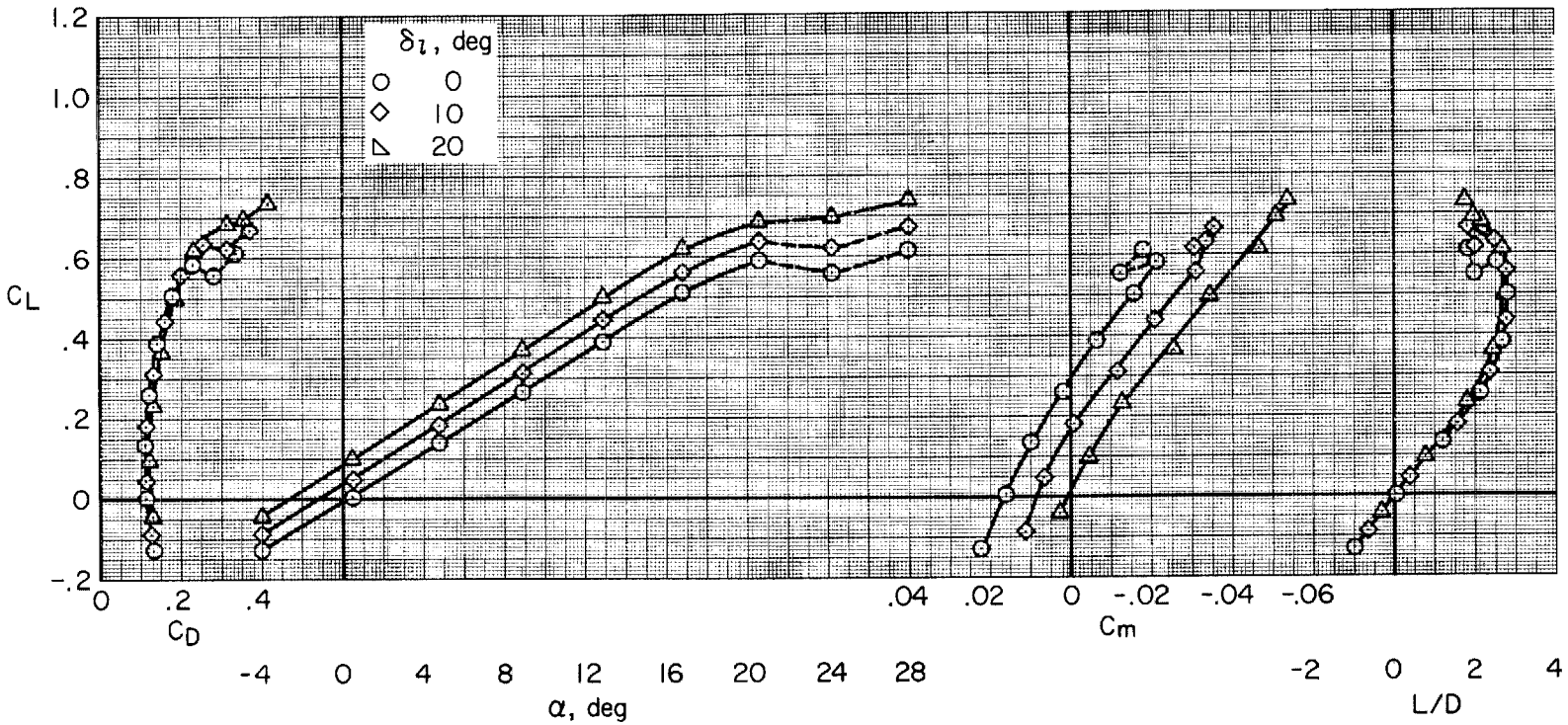

(c) $\delta_u = -20°$

Figure 8.- Continued.

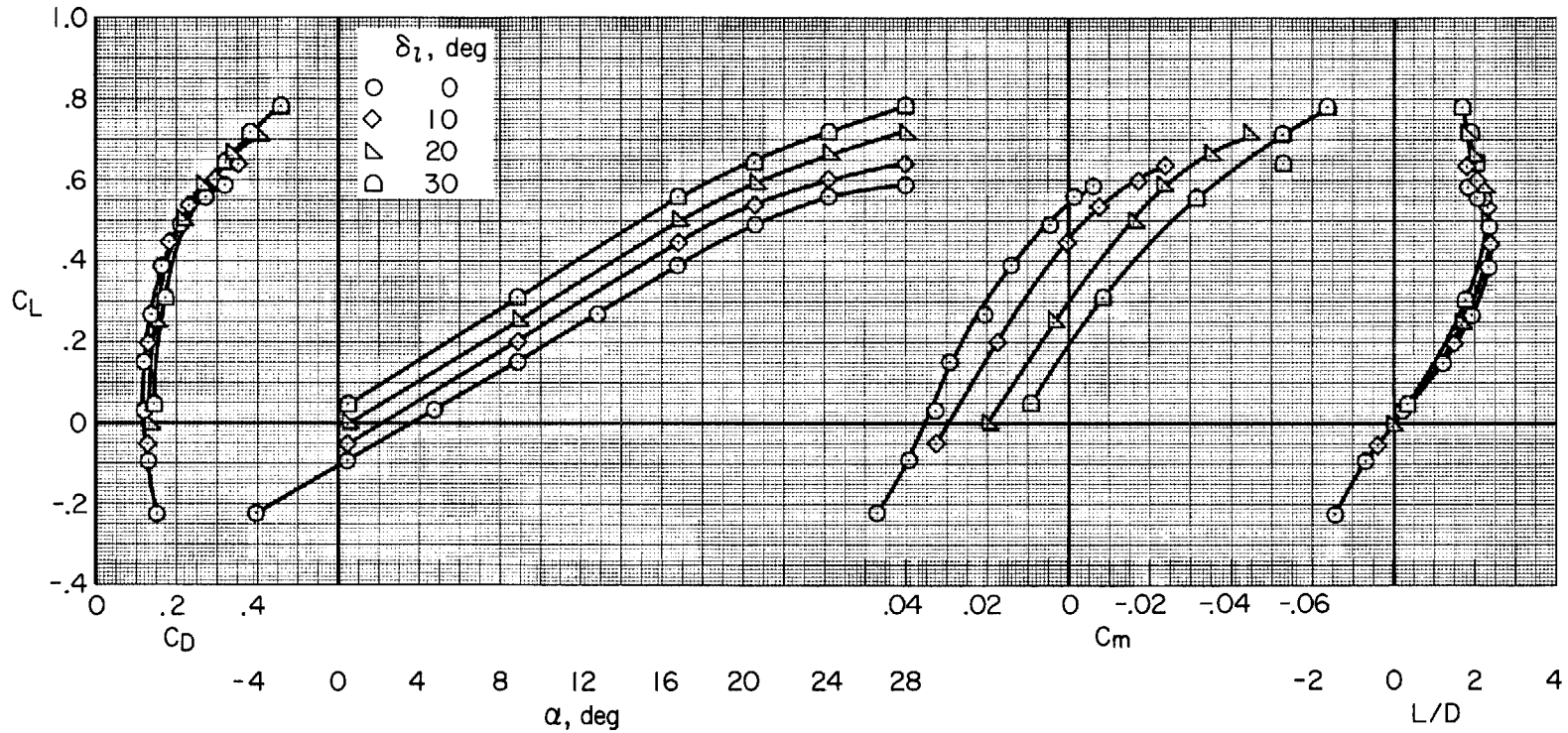

(d) $\delta_u = -30°$

Figure 8.- Concluded.

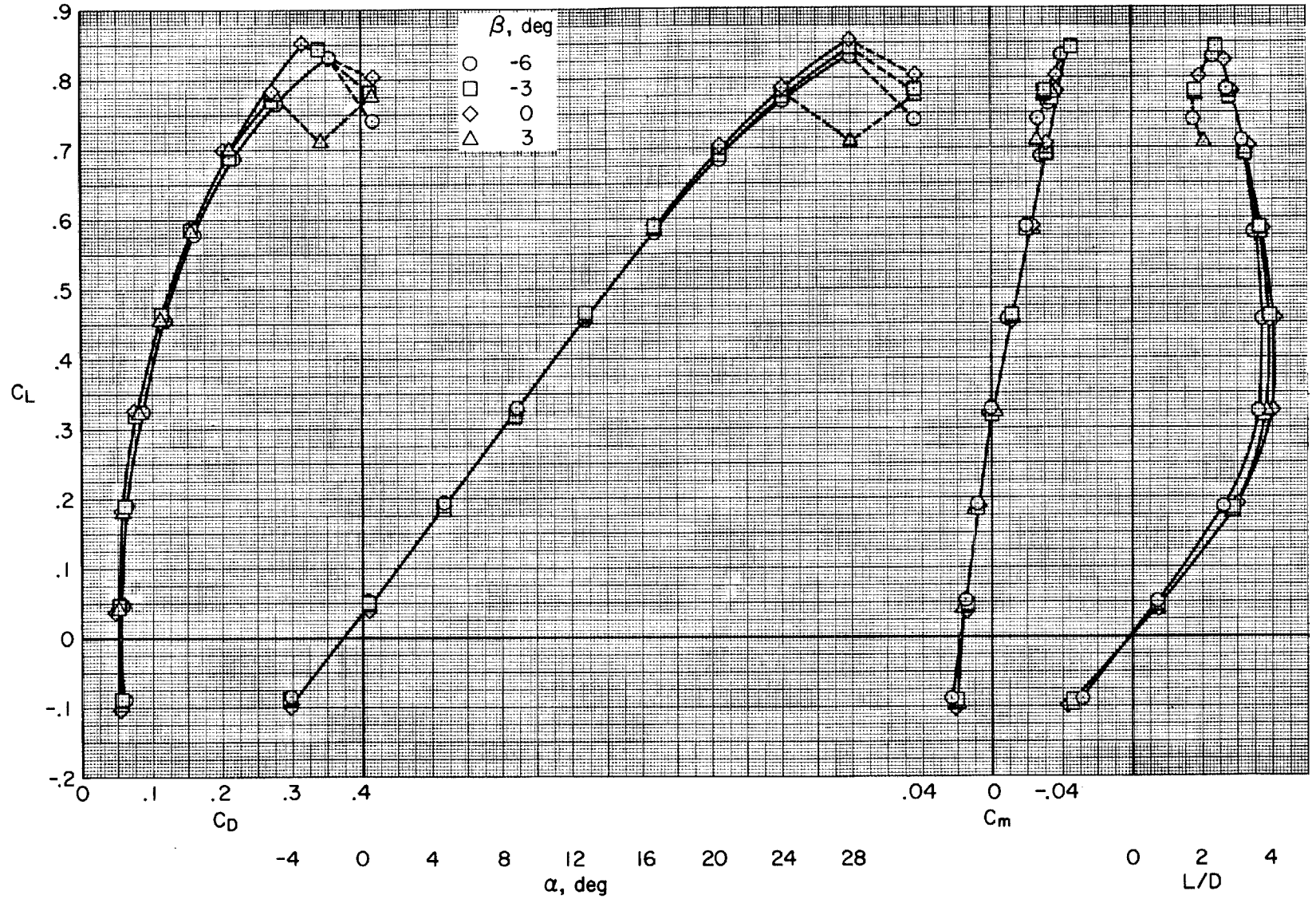

(a) Landing gear up.

Figure 9.- Effect of sideslip on longitudinal aerodynamic characteristics; $\delta_u = -20°$, $\delta_l = 10°$, $\delta_{rf} = -9°$.

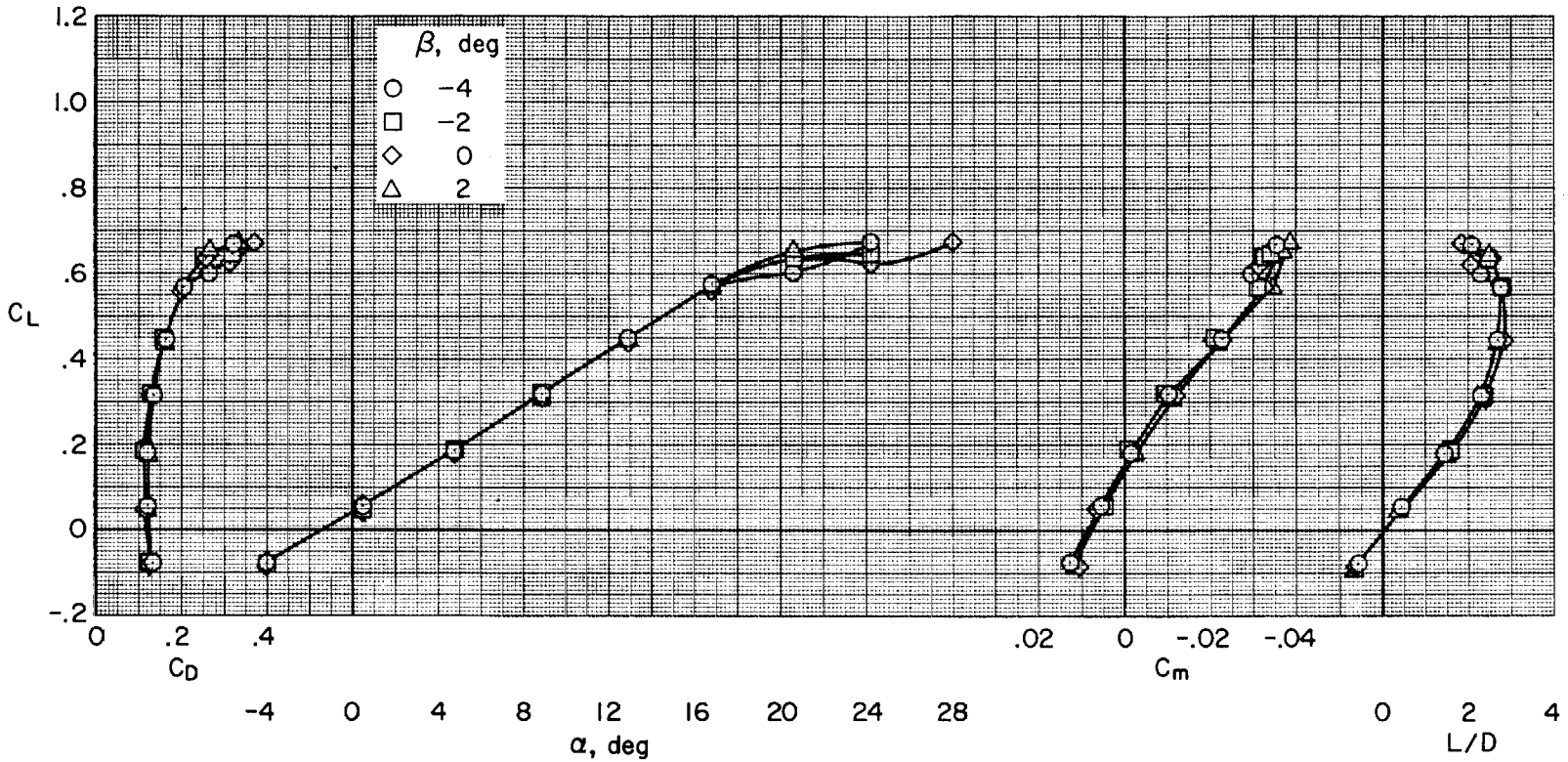

(b) Landing gear down.

Figure 9.- Concluded.

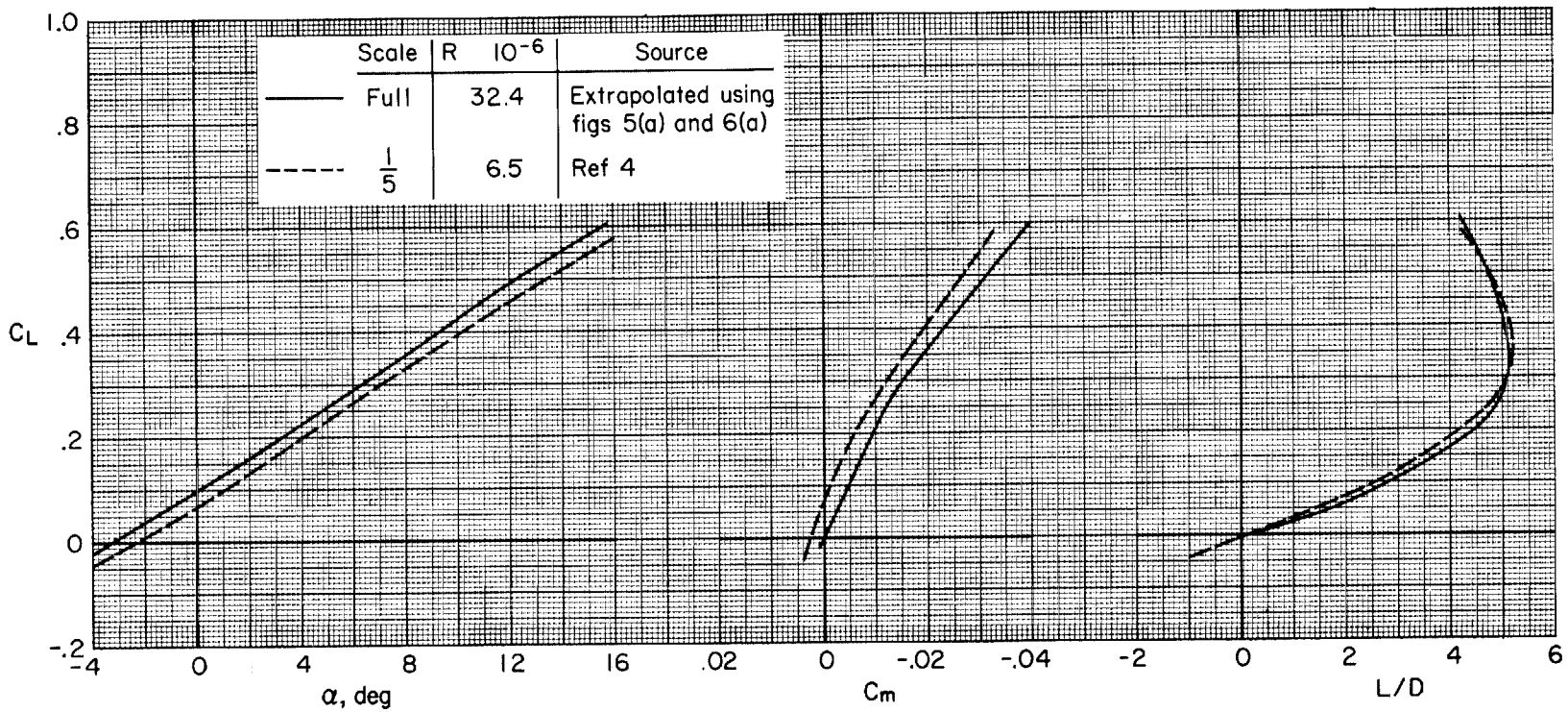

Figure 10.- Comparison of 1/5-scale results with estimated full-scale results at $\delta_u = -5°$, $\delta_l = 0°$, and $\delta_{rf} = -10°$.

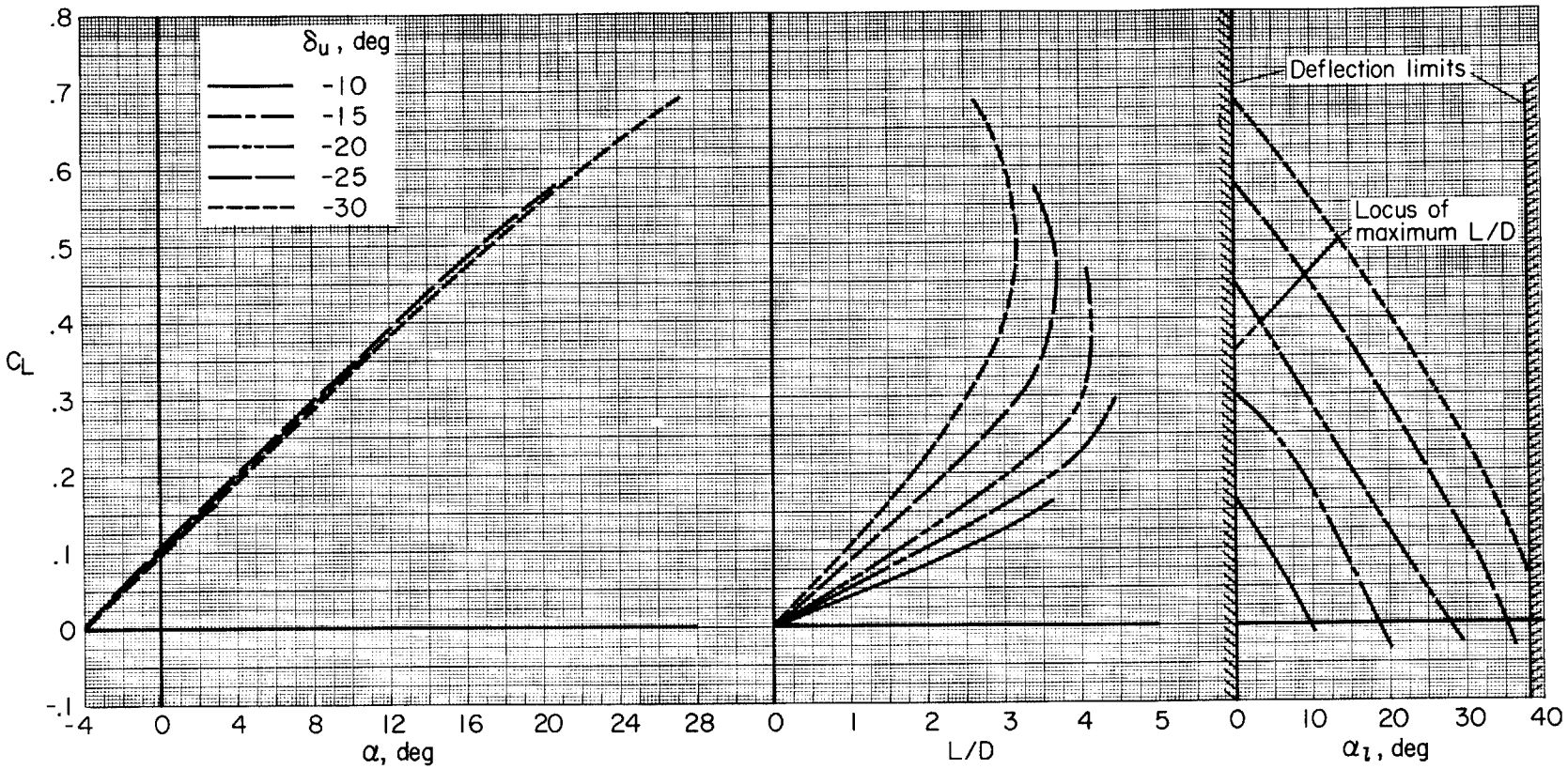

(a) Effect of upper flap setting with the landing gear up and $\delta_{rf} = -9°$.

Figure 11.- Trimmed ($C_m = 0$) aerodynamic characteristics.

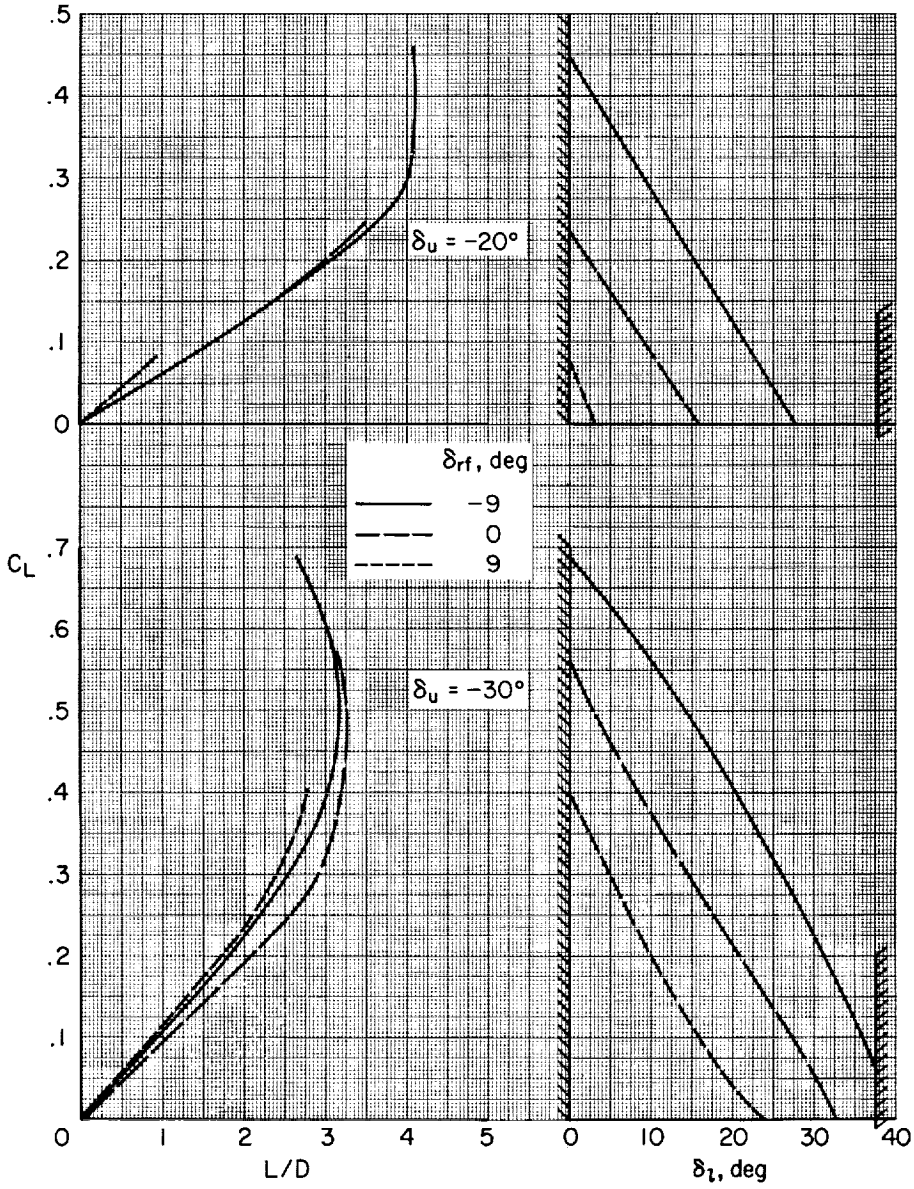

(b) Effect of rudder flare, δ_{rf}.

Figure 11.- Continued.

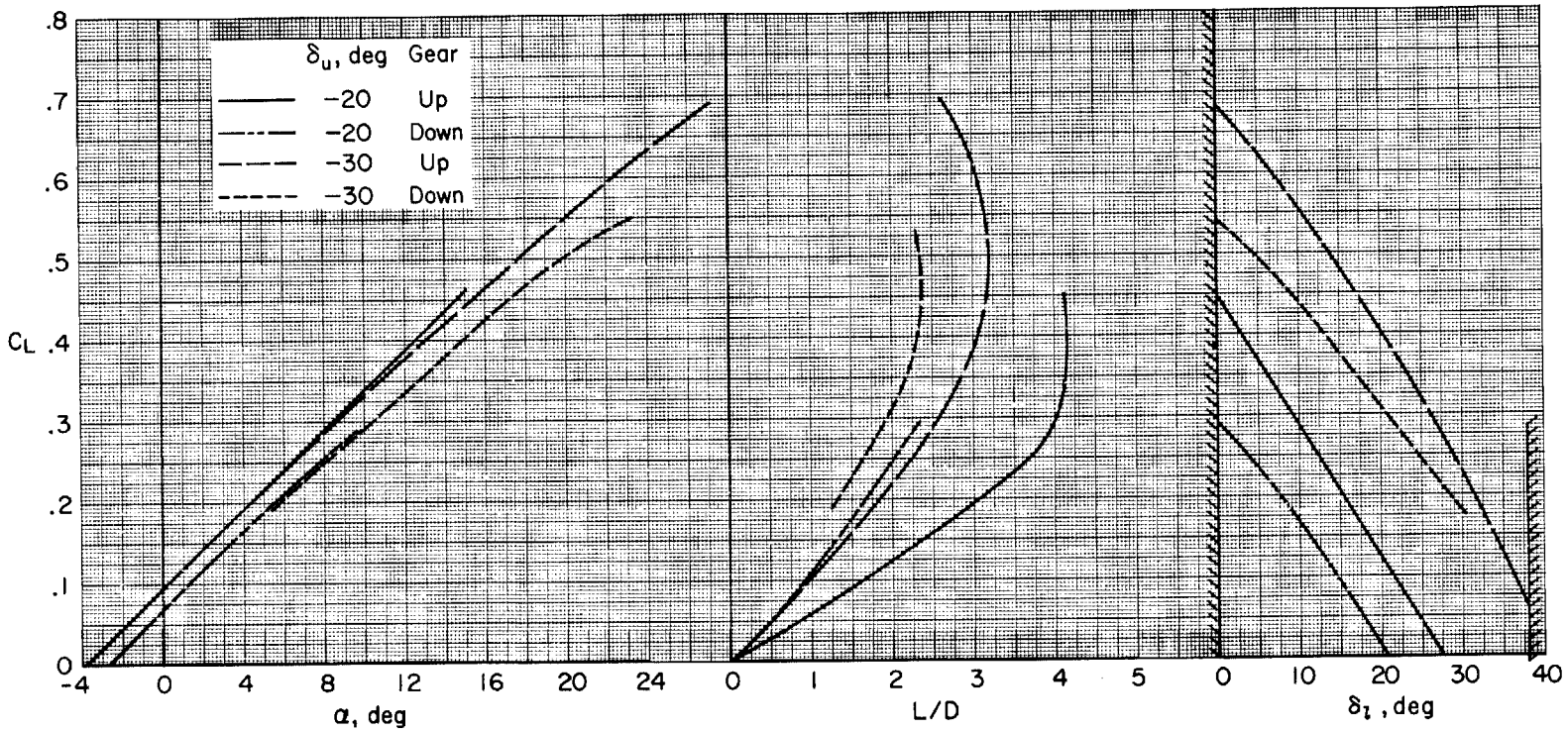

(c) Effect of landing gear with $\delta_{rf} = -9°$.

Figure 11.- Concluded.

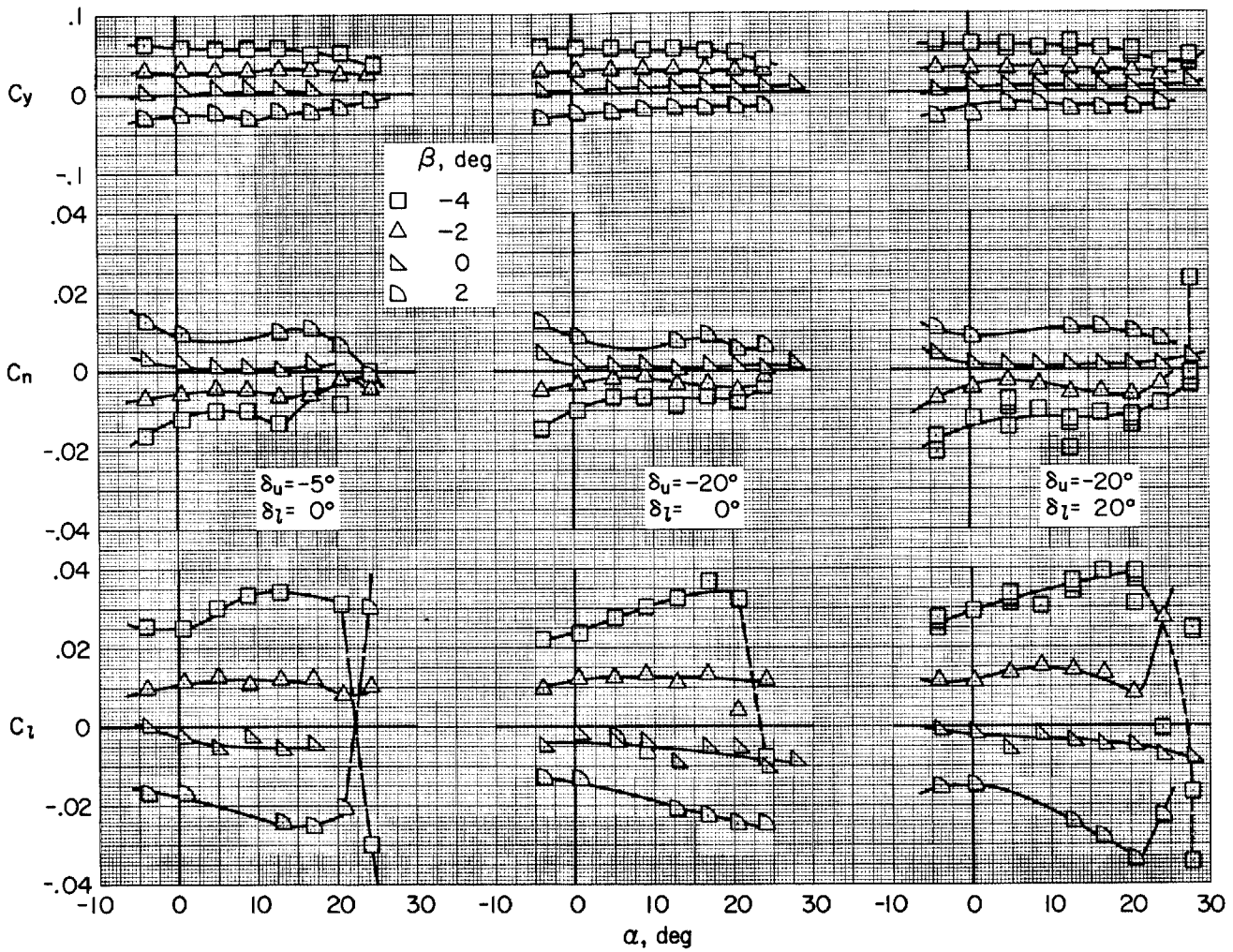

(a) Effect of longitudinal control setting with landing gear up and $\delta_{rf} = -9°$.

Figure 12.- Lateral-directional aerodynamic characteristics for several sideslip angles.

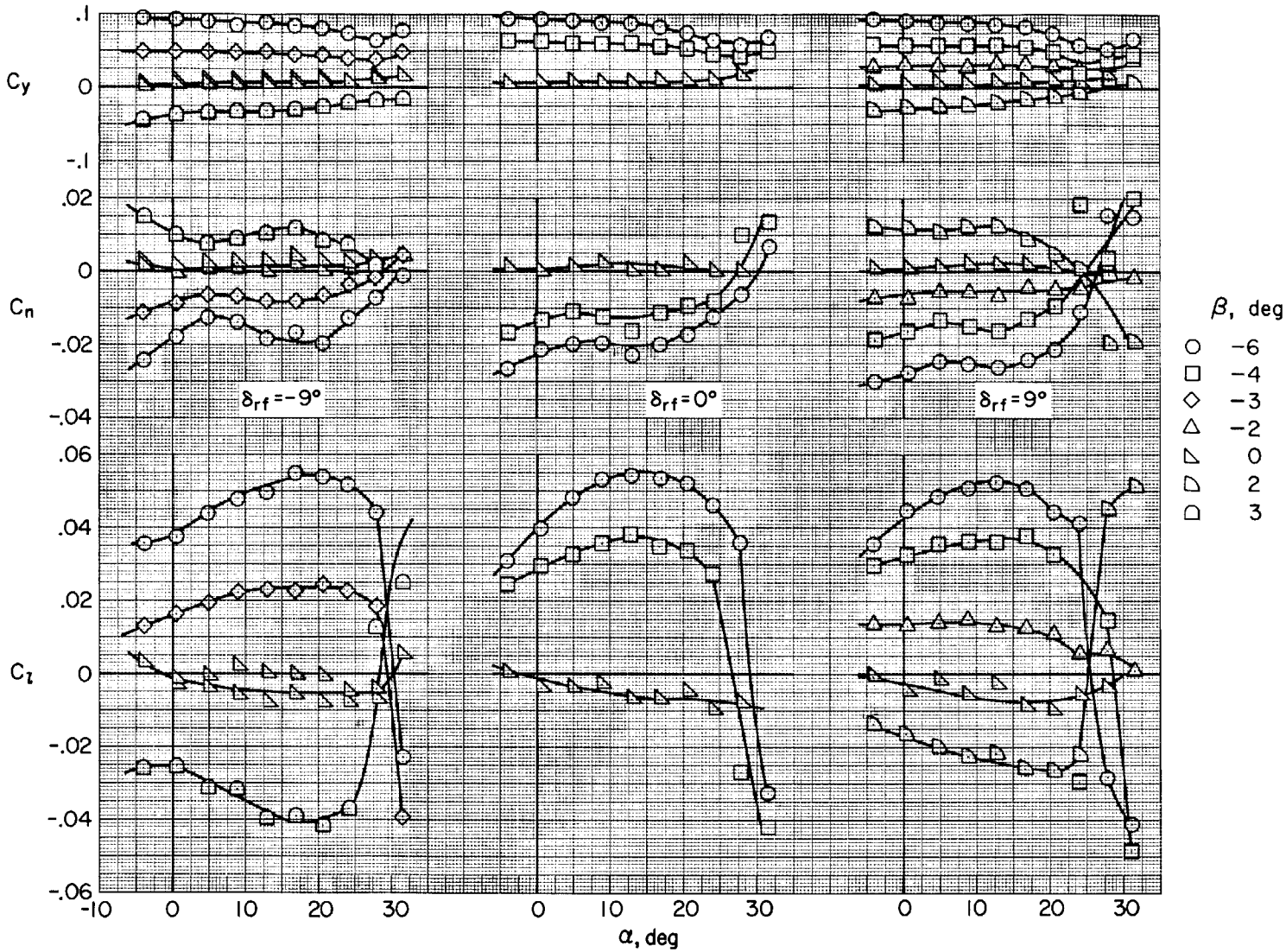

(b) Effect of rudder flare with landing gear up and $\delta_u = -20°$; $\delta_l = 10°$.

Figure 12.- Continued.

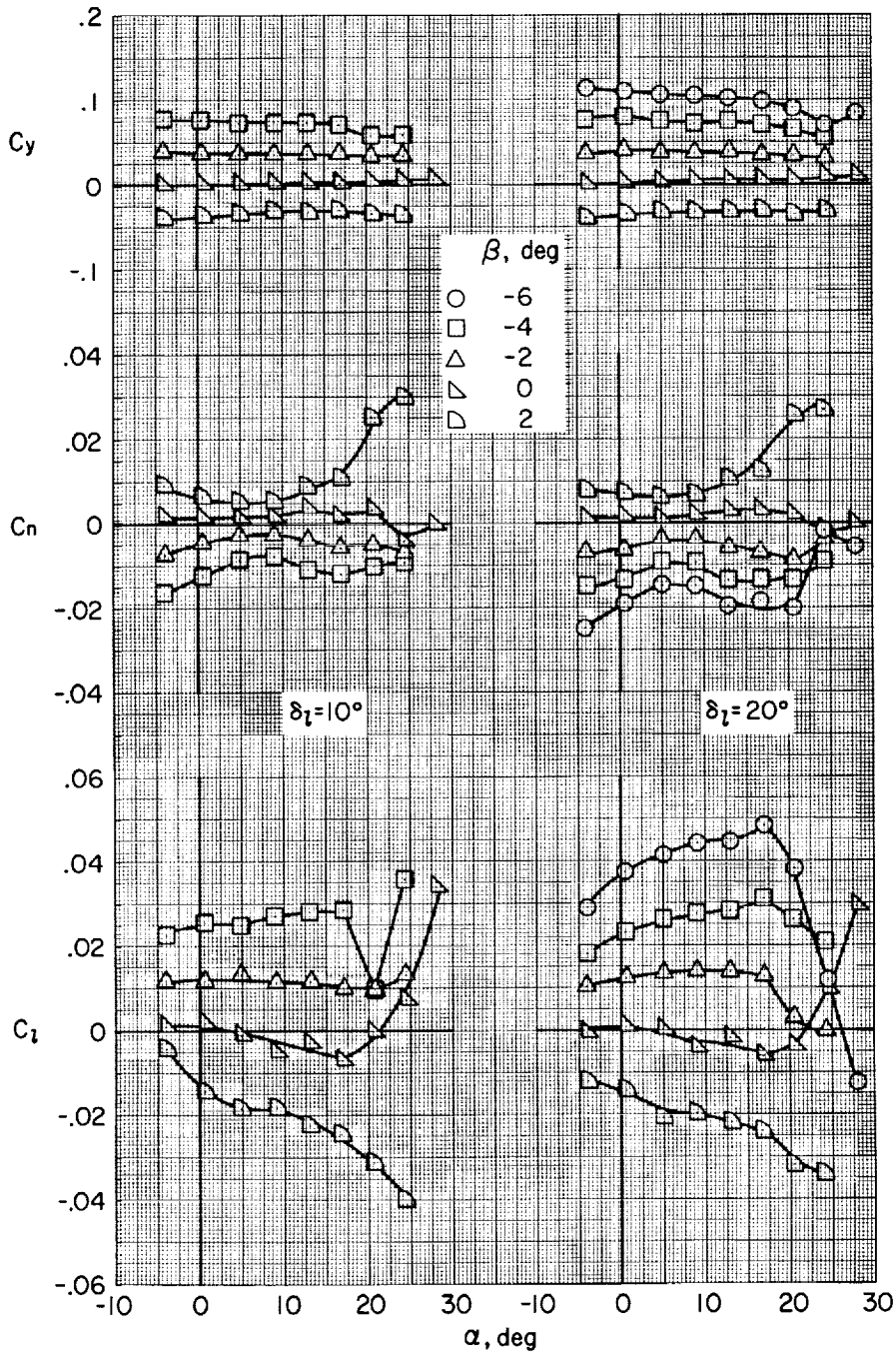

(c) Effect of lower flap setting with landing gear down and $\delta_u = -20°$ and $\delta_{rf} = -9°$.

Figure 12.- Concluded.

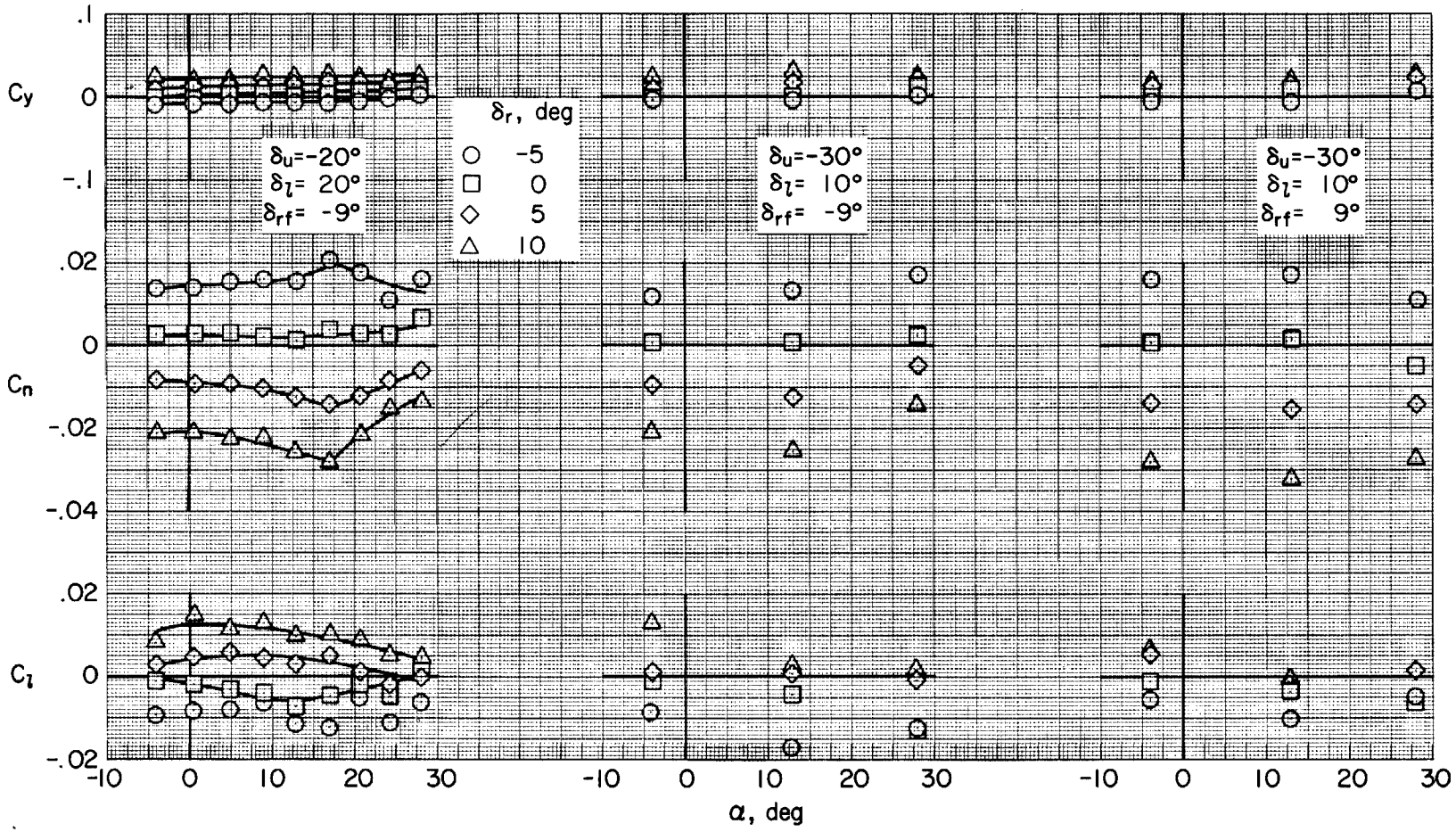

(a) Landing gear up.

Figure 13.- The effect of upper-rudder control on the lateral-directional aerodynamic characteristics; $\beta = 0°$.

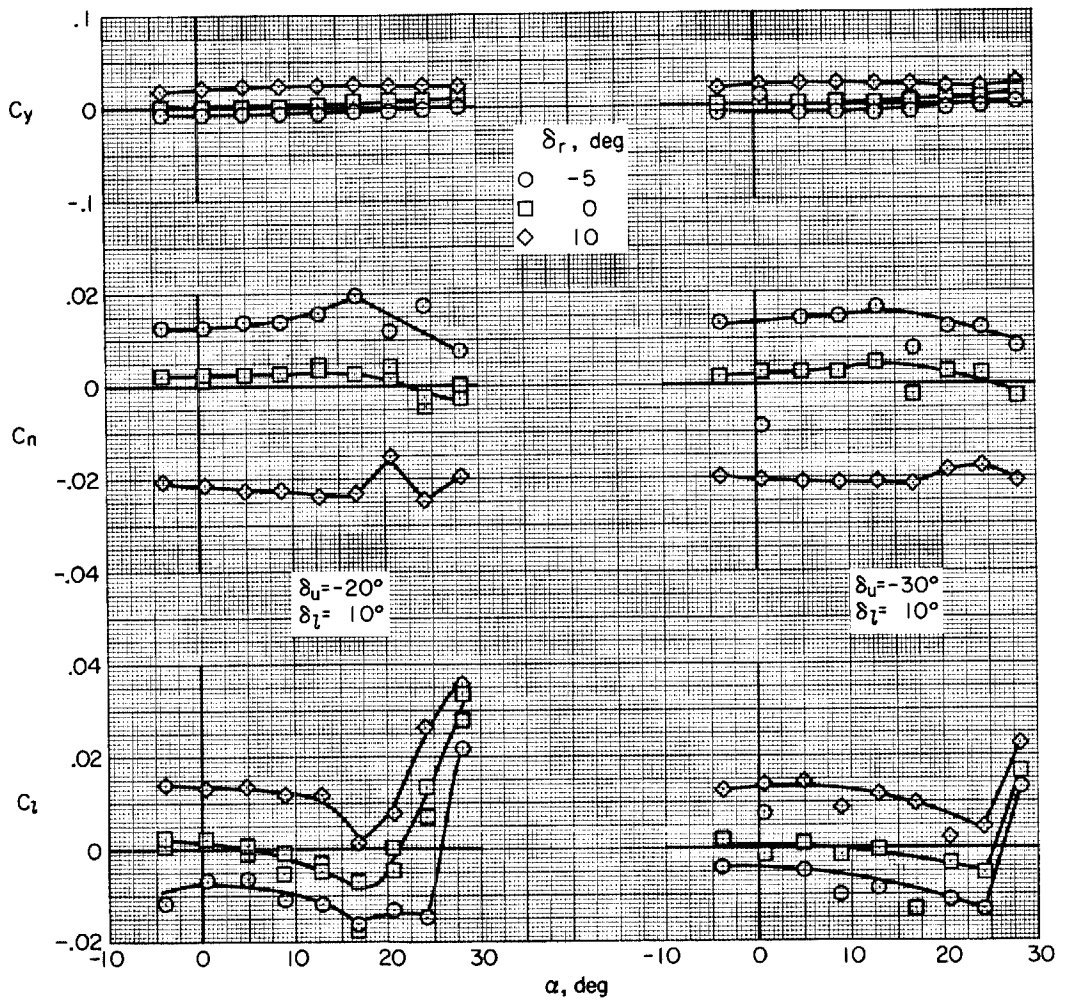

(b) Landing gear down and $\delta_{rf} = -9°$.

Figure 13.- Concluded.

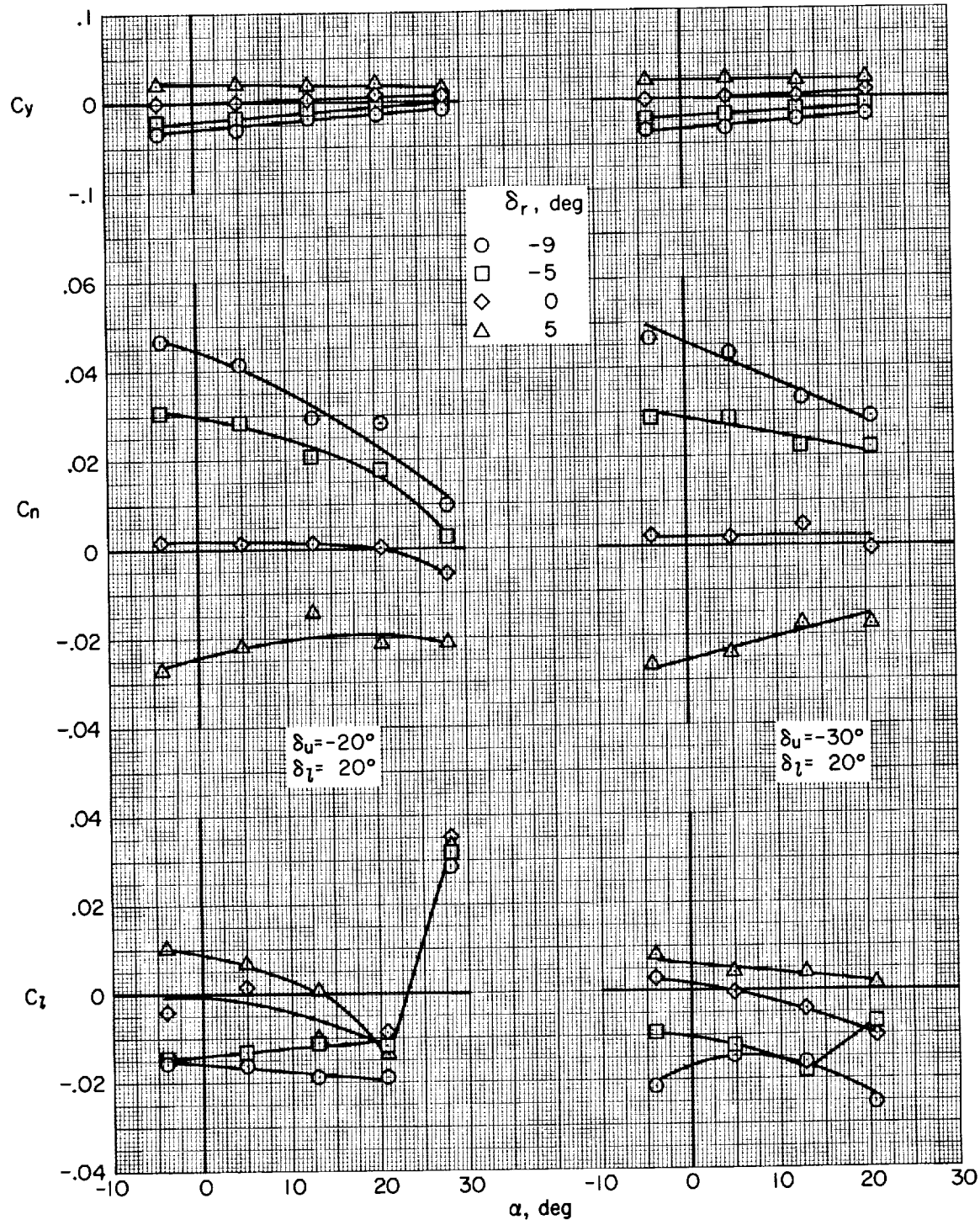

Figure 14.- The effect of lower rudder control on the lateral-directional aerodynamic characteristics with the landing gear down and $\delta_{rf} = 0°$.

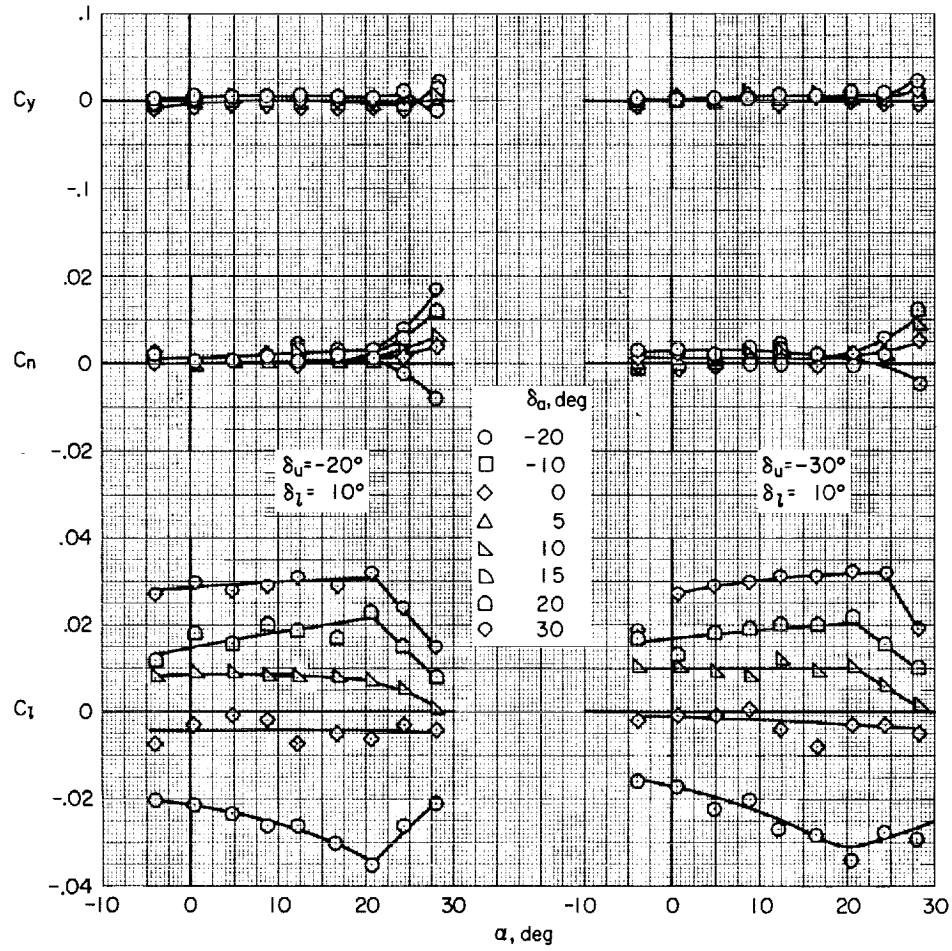

(a) Landing gear up and $\delta_{rf} = -9°$.

Figure 15.- Effect of differential upper flap deflection on the lateral-directional aerodynamic characteristics.

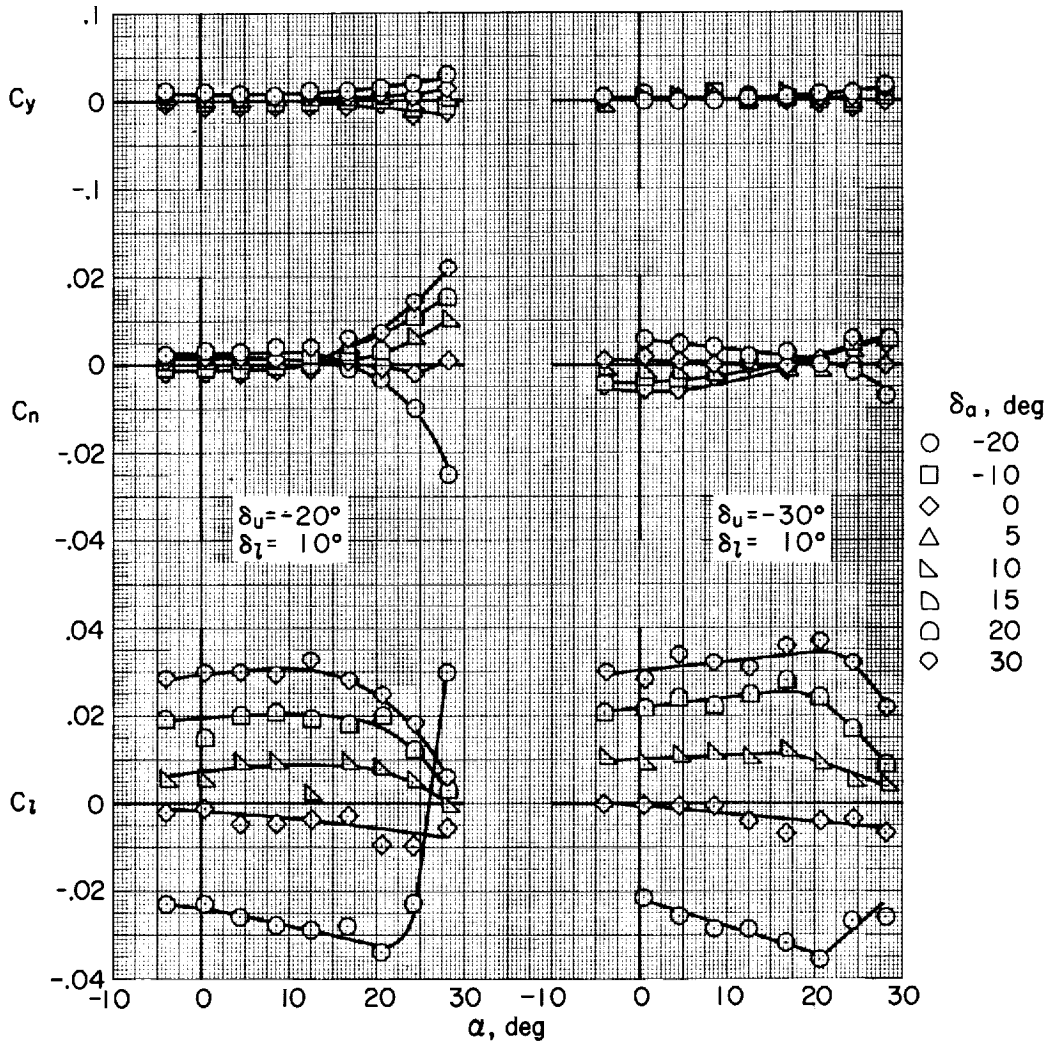

(b) Landing gear up and $\delta_{rf} = 0°$.

Figure 15.- Continued.

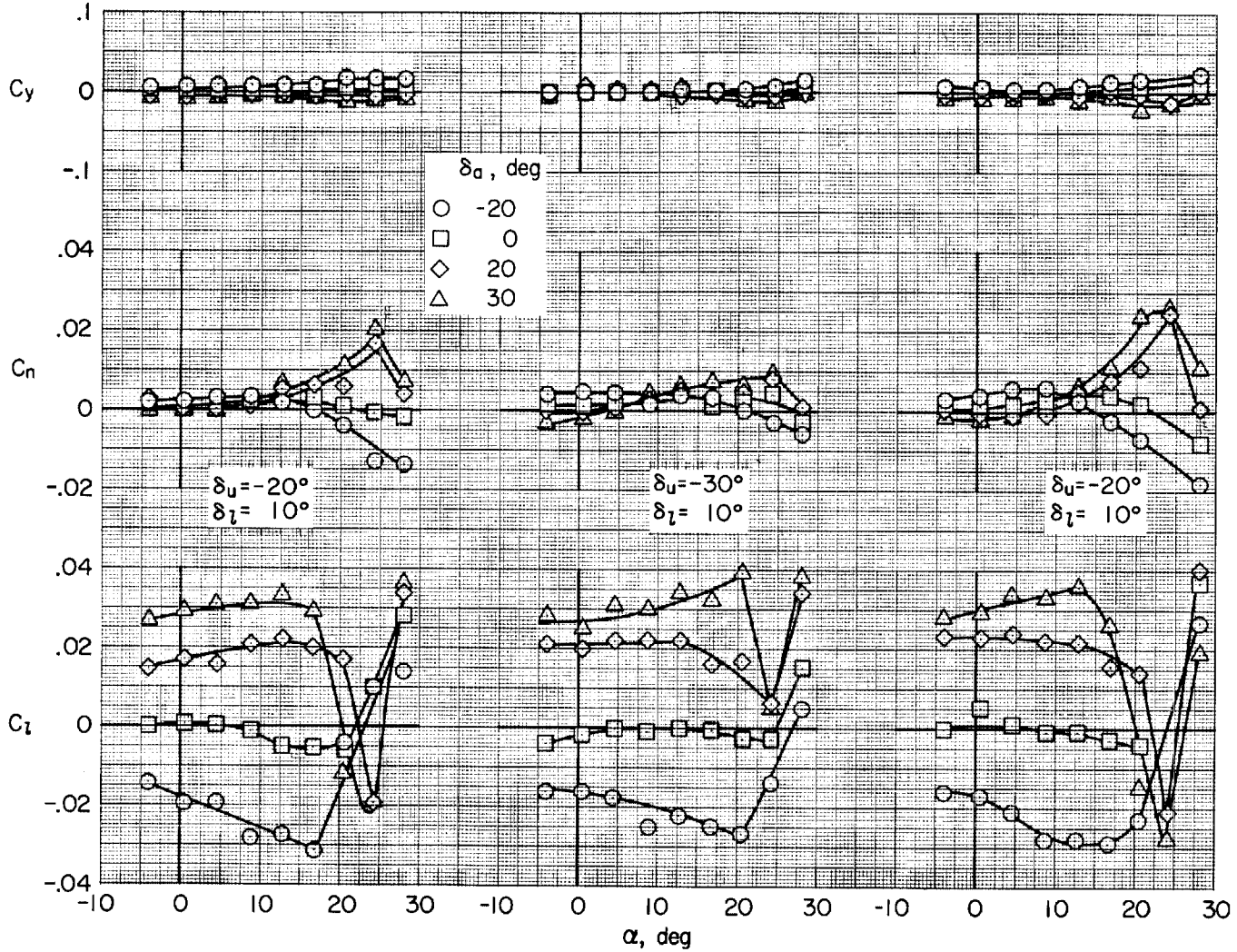

(c) Landing gear down and $\delta_{rf} = -9°$.

(d) Landing gear down and $\delta_{rf} = 0°$.

Figure 15.- Concluded.

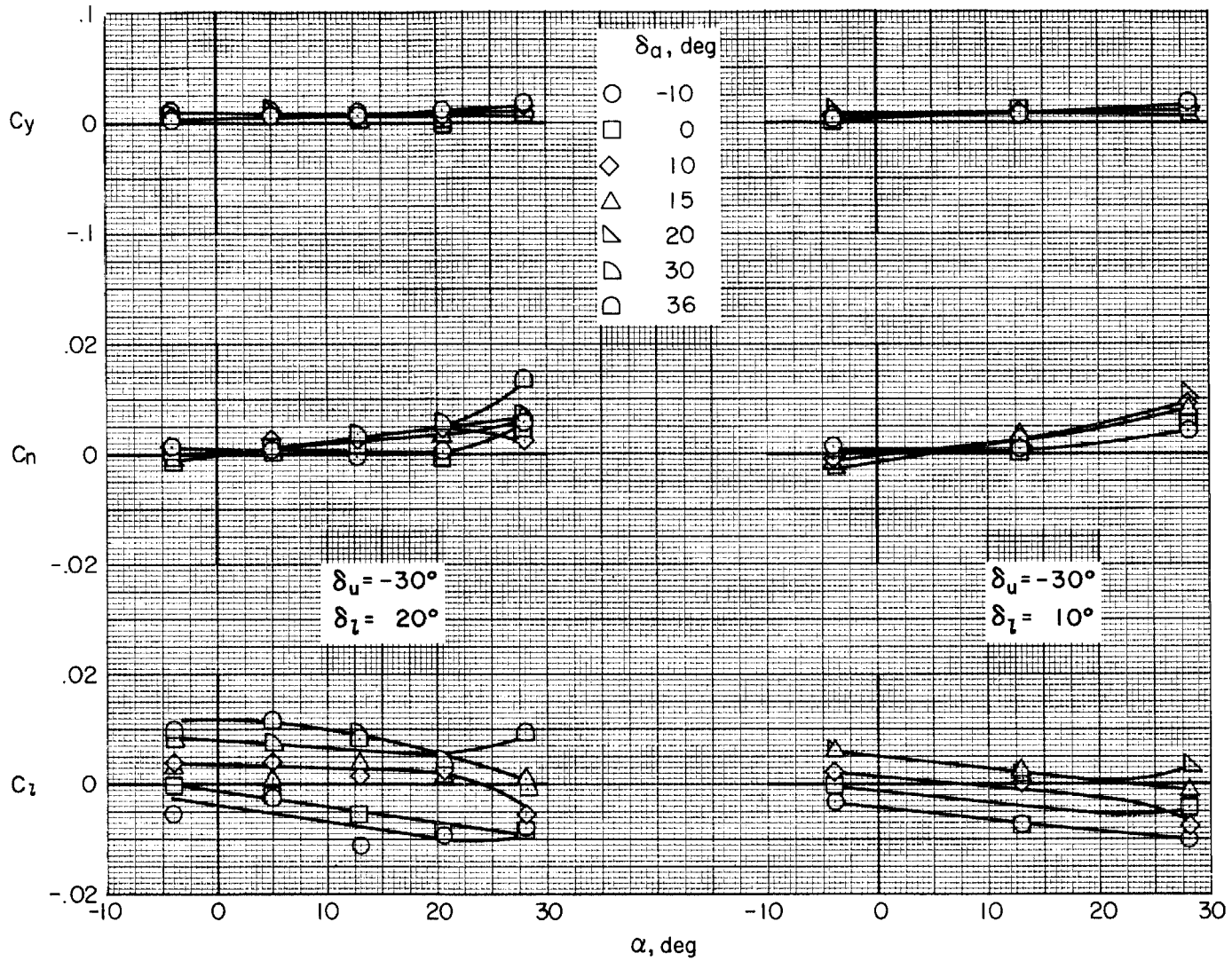

(a) Landing gear up.

Figure 16.- Effect of differential lower flap deflection on the lateral-directional aerodynamic characteristics; $\delta_{rf} = -9°$.

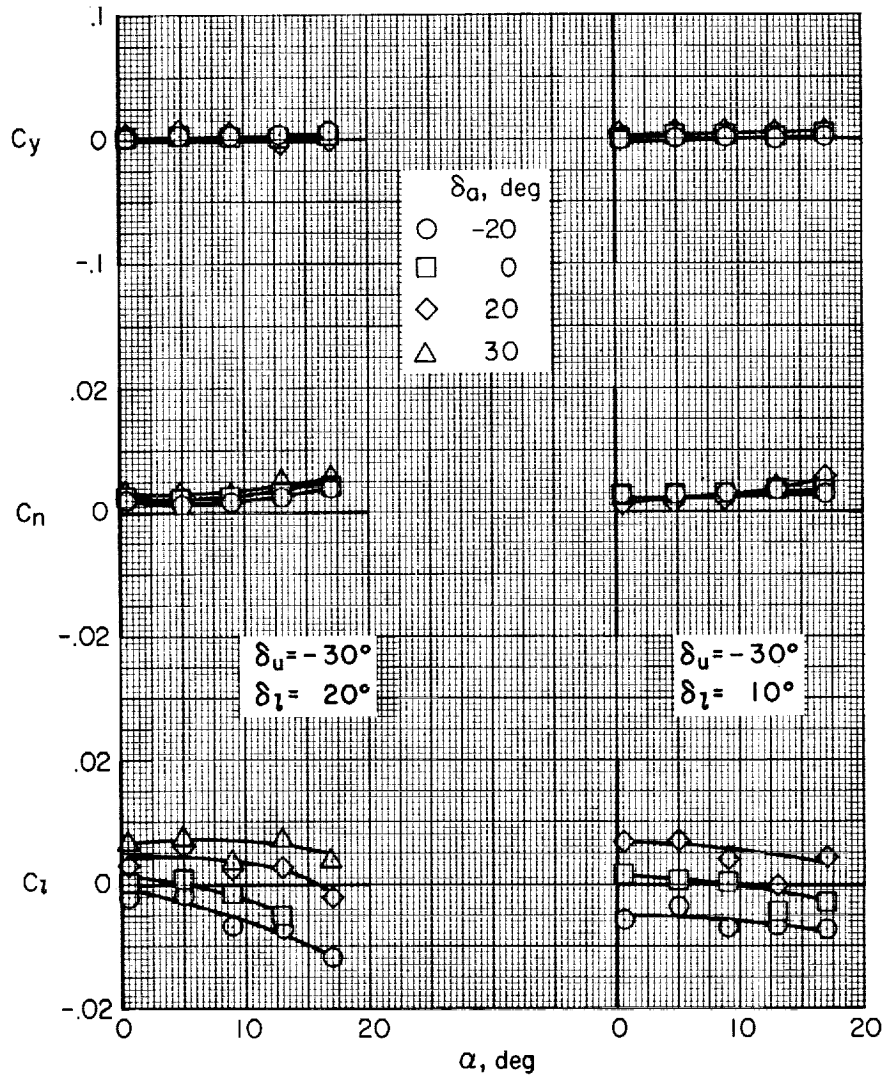

(b) Landing gear down.

Figure 16.- Concluded.

NASA-Langley, 1970 — 20 A-2823